Atmos. Meas. Tech. Discuss., 5, 5043–5105, 2012
www.atmos-meas-tech-discuss.net/5/5043/2012/
doi:10.5194/amtd-5-5043-2012

Atmospheric Measurement Techniques Discussions

Retrieval of tropospheric NO_2 columns from SCIAMACHY combining measurements from limb and nadir geometries

A. Hilboll[1], A. Richter[1], A. Rozanov[1], Ø. Hodnebrog[2], A. Heckel[3,1], S. Solberg[4], F. Stordal[2], and J. P. Burrows[1]

[1]Institute of Environmental Physics, University of Bremen, P.O. Box 330 440, 28334 Bremen, Germany
[2]University of Oslo, Oslo, Norway
[3]Department of Geography, Swansea University, Swansea, UK
[4]Norwegian Institute for Air Research, Kjeller, Norway

Received: 12 June 2012 – Accepted: 7 July 2012 – Published: 23 July 2012

Correspondence to: A. Hilboll (hilboll@iup.physik.uni-bremen.de)

Published by Copernicus Publications on behalf of the European Geosciences Union.

Abstract

Satellite measurements of atmospheric trace gases have proved to be an invaluable tool for monitoring the Earth system. When these measurements are to be used for assessing tropospheric emissions and pollution, as for example in the case of nadir measurements of nitrogen dioxide (NO_2), it is necessary to separate the stratospheric from the tropospheric signal.

The SCIAMACHY instrument offers the unique opportunity to combine its measurements in limb and nadir viewing geometries into a tropospheric data product, using the limb measurements of the stratospheric NO_2 abundances to correct the nadir measurements' total columns.

In this manuscript, we present a novel approach to limb/nadir matching, calculating one stratospheric NO_2 value from limb measurements for every single nadir measurement, abandoning global coverage for the sake of spatial accuracy. As a comparison, modelled stratospheric NO_2 columns from the Oslo CTM2 are evaluated as stratospheric correction, and both datasets are confronted with the originally used reference sector method.

Our study shows that stratospheric NO_2 columns from SCIAMACHY limb measurements very well reflect stratospheric conditions. The zonal variability of stratospheric NO_2 is captured by our matching algorithm, and the quality of the resulting tropospheric NO_2 columns improves considerably. Modelled stratospheric NO_2 columns from the Oslo CTM2 agree remarkably well with the measurements. Both datasets need to be matched to the level of the nadir measurements, however, because a time and latitude dependent bias between both stratospheric datasets and the measured nadir columns can be observed over clean regions. After accounting for this systematic bias between SCIAMACHY nadir observations and the stratospheric columns, both new stratospheric correction methods provide a significant improvement to the retrieval of tropospheric NO_2 columns from the SCIAMACHY instrument.

AMTD
5, 5043–5105, 2012

1 Introduction

For several decades, satellite-based instruments have been used to investigate the chemical composition of the Earth's atmosphere. Since the mid-1990s, the Global Ozone Monitoring Experiment (GOME, Burrows et al., 1999), the SCanning Imaging Absorption spectroMeter for Atmospheric CHartographY (SCIAMACHY, Bovensmann et al., 1999; Burrows et al., 1995, and references therein), the Ozone Monitoring Instrument (OMI, Levelt et al., 2006), and GOME's successor GOME-2 (Callies et al., 2000) have been launched in the class of nadir-viewing UV-vis instruments.

They all measure the solar radiation scattered in the atmosphere and reflected by the Earth's surface, in the UV/visible spectral region. While most of these instruments were originally designed to investigate the evolution of stratospheric ozone, their measurements allow for the analysis of a broad range of atmospheric constituents. One possible retrieval method is differential optical absorption spectroscopy (DOAS), a method based on the Beer-Lambert law which yields the quantity total slant column density (SCD_{tot}), the concentration of a specific absorber integrated along the effective light path through the atmosphere. These slant columns are then converted into vertical column densities (VCD) using so-called air mass factors (AMF), derived from radiative transfer calculations. A thorough description of the DOAS technique can be found in Platt and Stutz (2008), and an overview on the retrieval of trace gases form space is given in Burrows et al. (2011).

Several trace gases have been analysed with the DOAS technique, e.g. nitrogen dioxide (NO_2; among others: Richter and Burrows, 2002; Leue et al., 2001; Martin et al., 2002; Boersma et al., 2007), formaldehyde (Wittrock, 2006; de Smedt et al., 2010), bromine monoxide (Richter et al., 1998; Platt and Wagner, 1998; Chance, 1998), and iodine monoxide (Schönhardt et al., 2008). In this study, we focus on the retrieval of tropospheric NO_2. This particular trace gas is mainly emitted by anthropogenic activities; other sources include lightning (Beirle et al., 2004), biomass burning (Lee et al., 1997), and soil processes (Williams et al., 1992; Bertram et al., 2005). NO_2 plays a key role in tropospheric (as an important ozone precursor), as well as in stratospheric (being involved in ozone destruction) chemistry (Crutzen, 1979; Brasseur and Solomon, 2005). In both altitude regions, NO_2 quickly interchanges with nitric oxide (NO), which is why the sum of the two molecules is often referred to as NO_x. While anthropogenic emissions of NO cannot be directly monitored from space, the relatively short lifetime of the NO_2 molecule in the troposphere (between several hours and a few days, depending on atmospheric conditions) allows for the investigation of the spatio-temporal variability of NO_x emissions. Nitrous oxide (N_2O), which gets emitted at the surface mainly by microbial activity in soils, has a lifetime long enough to facilitate its transport into the stratosphere. There it reacts with an excited singlet D oxygen atom to produce two NO molecules (Brasseur and Solomon, 2005), forming the main source of stratospheric NO_2.

Since the DOAS method yields the trace gas' total slant column density, the investigation of its tropospheric abundance necessitates an additional information to separate the signal into its tropospheric and stratospheric components. Originally, this has been done using the reference sector method, in which the measurements taken in a region over the Pacific Ocean are assumed to include no tropospheric contribution (Richter and Burrows, 2002; Martin et al., 2002). The mean of these "clean" measurements is then subtracted from all measurements of the same day latitude-wise. Due to the low zonal variability of stratospheric NO_2 and the satellites' sun-synchronous orbit, the method usually yields reasonable results. However, this approximation sometimes leads to unphysical negative tropospheric column densities (SCD_{trop}), e.g. in areas affected by the polar vortex (see e.g. Fig. 4 top). This is the most visible sign that the assumption of zonal homogeneity is not always correct and shows the need to improve the quality of stratospheric NO_2 fields which are needed for investigating tropospheric NO_2 columns, especially their fine-scaled structures (Richter and Burrows, 2002; Boersma et al., 2004). Therefore, several other stratospheric correction schemes have been used to estimate the vertical stratospheric NO_2 columns (VCD_{strat}), namely (a) elaborating on the reference sector method by selecting a range of areas classified

Discussion Paper | Discussion Paper | Discussion Paper | Discussion Paper |

AMTD

5, 5043–5105, 2012

Tropospheric NO_2 from SCIAMACHY limb-nadir matching

A. Hilboll et al.

as unpolluted, (b) using a global chemistry and transport model (CTM), and (c) making use of independent measurements.

The earliest improvements with respect to the reference sector method have been suggested by Leue et al. (2001) and Wenig et al. (2004). In these studies, several regions around the globe have been classified as unpolluted, and a global stratospheric field of VCD_{strat} has been interpolated from the measurements over these regions. Later, Bucsela et al. (2006) further refined this method by using a wave-2 fit along zonal bands to estimate stratospheric NO_2 column densities over polluted regions. However, both methods suffer from the same drawback by requiring the definition of unpolluted regions, which can lead to too high estimates for VCD_{strat} in the case of a smooth tropospheric background signal, e.g. from soil emissions or large-scale biomass burning.

Regarding (b), a number of different approaches have been used to estimate stratospheric NO_2 columns. Stratospheric column densities from the SLIMCAT model adjusted to the measurements over the Pacific have been used by Richter et al. (2005), while Boersma et al. (2007) assimilate the satellite's NO_2 measurements over unpolluted regions into the TM4 model. This has the advantage of combining the absolute values from the measurements with the spatial distribution of the model. In this study, we investigate the use of stratospheric NO_2 columns from the Oslo CTM2 model, as described in Sect. 2.2.

As for (c), SCIAMACHY is the first instrument to combine limb- and nadir-mode measurements of approximately the same air mass, taken within 15 min of each other (Bovensmann et al., 1999). This offers the unique opportunity to use independent measurements done by the same instrument to investigate the stratospheric contribution to the total signal. The instrument detects the solar radiation scattered in the atmosphere and reflected by the Earth's surface. In nadir geometry, SCIAMACHY looks down towards the Earth's surface, and it measures total trace gas columns. In limb geometry, however, the instrument operates forward-looking and scans the atmosphere from the surface to a tangent height of 92 km (Gottwald and Bovensmann, 2011), thereby allowing the retrieval of vertical absorber profiles, using scattered light only.

This limb-nadir-matching has been exemplarily investigated in several studies (Sierk et al., 2006; Sioris et al., 2004). Beirle et al. (2010) have gone further and created a standard data product of stratospheric NO_2 for the extraction of the tropospheric NO_2 field by calculating a smoothed and interpolated global field from SCIAMACHY's limb-mode measurements.

In the present study, we use the SCIAMACHY limb-mode measurements in a different way, avoiding the smoothing and (most of the) interpolating steps taken by Beirle et al. (2010) by calculating VCD_{strat} for the locations of SCIAMACHY's nadir-mode measurements only. This is important because stratospheric NO_2 columns can show large day-to-day dynamical effects, especially in regions affected by the polar vortex, as shown by Dirksen et al. (2011). While this procedure, which is detailed in Sect. 2.3.1, yields the best possible matching of nadir and limb measurements, the stratospheric data product does not give daily global coverage, which means that this correction scheme is only suitable for SCIAMACHY measurements. The algorithm is tailored to provide a full dataset of tropospheric NO_2 from all available SCIAMACHY measurements from 2002 until the end of SCIAMACHY operations in 2012. Application of SCIAMACHY limb measurements as stratospheric correction is compared to the use of model simulations carried out with the Oslo CTM2 model, and the traditional reference sector method. This comparison is based on evaluation of (a) latitudinal and longitudinal variability of the derived stratospheric NO_2 fields and (b) the resulting fields of tropospheric NO_2.

2 Methods

In order to retrieve tropospheric NO_2 columns from SCIAMACHY measurements, first the total slant columns are calculated using the DOAS procedure. These total slant columns are subsequently corrected for the stratospheric contribution to the measurements, yielding SCD_{trop}.

AMTD
5, 5043–5105, 2012

For most practical applications, like the inversion of surface NO_2 emissions from the measurements, a cloud filter will be used to ignore cloud-covered scenes, and the resulting SCD_{trop} will be converted to vertical columns. These last retrieval steps lie however outside the scope of the present study and are further described in the literature (Richter et al., 2005; Nüß, 2005; Palmer et al., 2001; Martin et al., 2002; Boersma et al., 2004).

2.1 SCIAMACHY measurements

This present work concentrates on the step of converting the total to the tropospheric slant columns by using stratospheric NO_2 profiles retrieved from SCIAMACHY limb measurements as described in Sect. 2.1.2. First, as the SCIAMCHY limb retrieval is sensitive down to approximately 11 km, the stratospheric NO_2 profiles must be extrapolated downward to the tropopause layer. The resulting vertical profiles are then integrated into VCD_{strat}. In a next step, the limb measurements are geographically matched to the nadir measurements. We define the ground scene of a limb scan by the geolocation of the line of sight tangent point at the start and end of the state. Due to the elevation steps executed by the instrument, the tangent point of the line of sight moves towards the spacecraft as the platform moves along the orbit. The satellite's movement around the Earth thus leads to a rather narrow appearance of the along-track extent of the limb pixels (Gottwald and Bovensmann, 2011). While this small extent probably does not optimally reproduce the actual volume observed by the instrument, it is still the most plausible description not needing computationally expensive 3-D radiative transfer calculations (Puķīte et al., 2010). The small pixel sizes in along-track direction lead to relatively low global coverage, making the derivation of global fields from these measurements a challenging task.

In this study, we calculate one stratospheric NO_2 column for every single SCIAMACHY nadir measurement. Whilst having the disadvantage of not attaining global coverage with the resulting stratospheric data product, this procedure, which is detailed in Sect. 2.3.1, has the advantage of avoiding the need to average over several

Discussion Paper | Discussion Paper | Discussion Paper | Discussion Paper |
AMTD
5, 5043–5105, 2012
Tropospheric NO_2 from SCIAMACHY limb-nadir matching
A. Hilboll et al.

days of measurements, as, for example, in Beirle et al. (2010). In order to account for the sparser coverage of the limb measurements, we interpolate one VCD_{strat} for each measured nadir pixel, using the algorithm described in Sect. 2.3.1. The interpolated VCD_{strat} are then converted to slant columns using stratospheric air mass factors, as the subtraction of the stratospheric contribution on the total column measurements is performed for the measured slant columns. The air mass factor calculation is described in Sect. 2.3.2. Following this step, the limb stratospheric slant columns are matched to the SCD_{tot} from nadir measurements. The rationale for this matching, which is achieved via an additive offset, will be described in Sect. 2.3.4. The full procedure is depicted in Fig. 1.

2.1.1 Retrieval of total slant columns from nadir measurements

To calculate total slant column densities from the spectra measured by SCIAMACHY, the NO_2 absorption averaged over all light paths contributing to the signal is determined using the Differential Optical Absorption Spectroscopy (Platt and Stutz, 2008) method in the 425–450 nm wavelength region (Richter and Burrows, 2002). Additionally to NO_2, the trace gases O_3, O_4, and H_2O are included in the fitting procedure. The NO_2 and O_3 absorption cross-sections used in the fitting procedure have been measured at 243 K (Bogumil et al., 2003). Furthermore, a synthetic Ring spectrum (Vountas et al., 1998), an undersampling correction (Chance, 1998), and a calibration function accounting for the polarisation dependency of the SCIAMACHY spectral response are included in the fit. A polynomial of degree 3 is included to account for low frequency variations of the optical density, for example from scattering.

2.1.2 Limb profiles

The limb-mode measurements made by SCIAMACHY are the most elaborate global assessment of stratospheric NO_2 available today. They provide a vertical NO_2 profile from 11 km up to 46 km, with a vertical sampling of 1 km and a vertical resolution of

AMTD
5, 5043–5105, 2012

3–5 km. Each instrument swath is divided into four distinct limb states, yielding a cross-track pixel size of 240 km each. About 100 limb NO_2 profiles are taken by SCIAMACHY per orbit. In this study, we use the NO_2 concentration profiles from the IUP Bremen scientific retrieval, version 3.1 (Bauer et al., 2012). For measurements with the tropopause altitude lower than the 11 km lower boundary of the SCIAMACHY limb profiles, the profiles were extended down towards the tropopause by NO_2 concentration profiles derived from a monthly climatology created from the Oslo CTM2 model run (see Sect. 2.2).

2.1.3 Tropopause altitude

The tropopause height was computed from the ECMWF ERA-Interim reanalysis (Dee et al., 2011), which is on a latitude/longitude grid of 1.5° resolution and has 6-hourly output. The location of the tropopause was obtained by applying both dynamical (potential vorticity) and thermal (lapse rate) definitions, following an approach similar to the one discussed in Hoinka (1998). The combination of the dynamical and thermal criteria enables a clear definition of the boundary between the troposphere and the stratosphere. For the tropics we applied the thermal criterion and from the mid-latitudes to the poles we applied the dynamical criterion using a potential vorticity of 3 PVU ($1\,\text{PVU} = 10^{-6}\,\text{km}^2\,\text{s}^{-1}\,\text{kg}^{-1}$). In the transition region between the two regimes both criteria were used and weighted with the distance from the regime boundaries. This method is further described in Ebojie et al. (2012).

2.2 Oslo CTM2 simulations

Since appropriate profile measurements are not available, model simulations are used to obtain quantities for verification purposes. The NO_2 vertical profiles and tropospheric column NO_2 values have been validated independently (Bauer et al., 2012; Heue et al., 2005; Richter et al., 2004). Additionally, model simulations have to be used to estimate the tropospheric background signal (see Sect. 2.3.5).

In this study, we use NO_2 columns modelled by the Oslo CTM2 model (Søvde et al., 2008). The model is driven by meteorological data from the ECMWF Integrated Forecast System (IFS) model, and has been run with both tropospheric (Berntsen and Isaksen, 1997) and stratospheric (Stordal et al., 1985) chemistry for the period 1997–2007, whereof the latter ten years have been used in the analysis (1997 was considered as spin-up). It extends from the surface to 0.1 hPa in 60 vertical layers, and a horizontal resolution of Gaussian T42 ($2.8125^\circ \times 2.8125^\circ$) has been used; the time step is 60 min. Anthropogenic emissions are taken from the MACCity inventory (Granier et al., 2011), while biogenic emissions are from POET (Granier et al., 2005). Biomass burning emissions are from RETRO (Schultz et al., 2008) for 1997–2000 and from GFEDv2 (van der Werf et al., 2006) for the remaining period (World Meteorological Organization, 2007). Lightning emissions are based on Price et al. (1997) and re-distributed according to lightning frequencies; the procedure is described in detail in Søvde et al. (2008). Advection in Oslo CTM2 is done using the second order moment scheme (Prather, 1986), convection is based on the Tiedtke mass flux parametrisation (Tiedtke, 1989), and boundary layer mixing is treated according to the Holtslag K-profile method (Holtslag et al., 1990). The Quasi Steady-State Approximation (Hesstvedt et al., 1978) is used for the numerical solution in the chemistry scheme, and photo-dissociation is done online using the FAST-J2 method (Wild et al., 2000; Bian and Prather, 2002).

Vertical stratospheric NO_2 columns are calculated by integrating the modelled concentrations from the tropopause to the top of the modelled atmosphere at 0.1 hPa. For this purpose, the tropopause height is fixed to the layer interface which is closest to the “real” tropopause altitude calculated using the 2.5 PVU criterion. Compared to the hybrid criterion used in the calculation of measured stratospheric columns (see Sect. 2.1.3), this only leads to minor differences due to the strong vertical gradient in the PV field near the tropopause.

AMTD
5, 5043–5105, 2012

2.3 Applying stratospheric correction

2.3.1 Interpolation to nadir measurement location

Both the model and the limb stratospheric NO_2 column products used in this study are only available on a horizontal resolution which is much coarser than the spatial extents of individual SCIAMACHY nadir measurements ($60 \times 30\,\mathrm{km}^2$). Therefore, we need to interpolate the coarse stratospheric columns to the locations of each SCIAMACHY nadir measurement, to ensure the best possible spatial matching.

For SCIAMACHY limb measurements, several steps are required in order to calculate stratospheric NO_2 columns for each nadir measurement, processing each orbit separately. First, we assign a fixed azimuth (line of sight) angle to each of the four discrete limb states, namely -25°, -8°, 10° and 27°. These angles are chosen to be the mean viewing azimuth angles of those nadir pixels which fall into the viewing direction of the respective limb state.[1]

Next, we consider the stratospheric NO_2 column density along every state as depending on latitude only. For all nadir pixels n, we calculate a stratospheric column C_i^n by linearly interpolating along-track, that is along each limb state i. For both limb and nadir measurements, we only take into account the descending parts of the orbit to avoid complications from measurements taken at different local times and therefore photochemical states. This yields four distinct values for every nadir state n, i.e. one for each limb state. Finally, for all nadir pixels n, we consider the stratospheric NO_2 column to be a function of the line of sight, and linearly interpolate the correct column density from the four column densities C_i^n previously calculated. This procedure is illustrated in Fig. 2.

[1] In this case a negative angle describes a point east of the nadir point, while a positive angle describes a location west of the nadir point.

In the case of Oslo CTM2 simulations, the modelled NO_2 columns are interpolated to the location and time of the individual nadir measurements using smoothing cubic splines and linear interpolation, respectively.

2.3.2 Stratospheric air mass factor (AMF)

In order to convert the VCD_{strat} to slant columns, stratospheric air mass factors (AMF) need to be calculated. Here, we use the radiative transfer model SCIATRAN (Rozanov et al., 2005b) to calculate a block air mass factor (BAMF) table for 31 solar zenith angles (SZA) between 10° and 92°, and for 101 equally spaced altitude layers from sea level (0 km) to 100 km. The NO_2 profile has then been interpolated to the altitude layers of the BAMF table.

2.3.3 Correcting for the temperature-dependence of the NO_2 absorption cross-section

The retrieval process for the NO_2 profiles from SCIAMACHY limb measurements accounts for the temperature-dependence of the NO_2 absorption cross-section using temperature fields from the ECMWF ERA-Interim reanalysis (Dee et al., 2011). In the DOAS fits applied to the measured nadir radiances, however, a cross-section measured at a fixed temperature of 243 K has been used. We therefore implemented a correction based on the idea presented in Boersma et al. (2004).

Nüß et al. (2006) calculated scaling factors by comparing differential cross-sections measured at four distinct temperatures between 221 K and 293 K. In this study, we assume a linear relation of the cross-section on temperature. From the ERA-Interim reanalysis, we extract a vertical temperature profile for each individual SCIAMACHY limb state and interpolate it to the vertical grid used in the BAMF calculation. Next, we calculate one scaling factor for each altitude layer, using the interpolated temperature profile and the scaling factors derived by Nüß et al. (2006). These scaling factors are then applied to the NO_2 profile before calculating stratospheric air mass factors

AMTD
5, 5043–5105, 2012

using the BAMF table. The stratospheric air mass factor for the limb state is then linearly interpolated to the correct SZA. Finally, the air mass factors are interpolated to the individual nadir measurements using the same procedure as in the case of the stratospheric NO_2 columns from the limb measurements (see Sect. 2.3.1).

2.3.4 Offset limb-nadir

When comparing, over clean regions, the interpolated SCD_{strat} from the limb measurements to the SCD_{tot} derived from SCIAMACHY nadir measurements, one can observe a latitude- and time-dependent offset between the two datasets (see Fig. 6). In order to account for these systematic biases, we apply a daily, latitude-dependent offset to all interpolated limb-mode SCD_{strat}. For this purpose, zonal means of nadir SCD_{tot} and limb SCD_{strat} over the Pacific Ocean (180° W–150° W) are calculated in steps of 0.125° latitude, and the difference between the two datasets is then added to each interpolated limb-mode SCD_{strat}. The application of this bias correction to account for systematic differences between limb and nadir measurements is in accordance with Beirle et al. (2010), who dealt with the problem similarly using their "Relative limb correction". Possible reasons behind the observed offset are discussed in Sect. 3.2.2.

An equivalent correction has been applied to the Oslo CTM2 simulated VCD_{strat} to account for differences between measured and modelled stratospheric NO_2 fields.

2.3.5 Pacific background

By applying the aforementioned offset to the retrieved limb SCD_{strat}, we assume that there are no significant tropospheric quantities of NO_2 in the reference sector. Therefore, the SCD_{trop} obtained by subtracting SCD_{strat} from SCD_{tot} must be corrected for the tropospheric NO_2 background levels. As ground-based measurements of tropospheric NO_2 over the Pacific Ocean are extremely sparse, and we need to apply this correction for all latitudes, we chose to use climatological NO_2 data derived from model simulations. Here, we use a climatology of monthly mean values derived from the Oslo CTM2 model (see Sect. 2.2). Similar corrections have been previously performed by Martin et al. (2002). The modelled VCD_{trop} are converted to slant columns using a monthly climatology of tropospheric air mass factors, which are calculated using the radiative transfer model SCIATRAN and NO_2 profiles from the MOZART4 model. Details about the used air mass factors can be found in Nüß (2005).

2.3.6 Reference sector method

Originally, the stratospheric correction scheme applied in most cases has been the so-called reference sector method. It is the most simple of the available stratospheric correction schemes and based on the nadir measurements alone.

The reference sector method relies on the assumptions that (a) longitudinal variations of stratospheric NO_2 are negligible, and that (b) there is no tropospheric NO_2 in a reference sector above the Pacific Ocean. The global field of stratospheric slant columns is then approximated by taking the average of all total slant columns within a 0.125° latitude band over the reference sector, and taking this value as constant for all points of the same latitude. The exact geographical definition of the reference sector depends on implementation; in this study, the region between the longitudes 180° W and 150° W is used. Finally, the tropospheric background signal as modelled by Oslo CTM2 is added to the tropospheric slant columns (see Sect. 2.3.5).

3 Results and discussion

3.1 Spatial variability of stratospheric NO_2 columns

The underlying assumption of the reference sector method is the zonal homogeneity of stratospheric NO_2. Figure 3 shows monthly mean VCD_{strat} NO_2 from SCIAMACHY limb measurements for June 2010. As it can be seen, the zonal variability is far from negligible, indicating the inadequacy of the reference sector method in many situations.

AMTD
5, 5043–5105, 2012

This becomes apparent in the distribution of tropospheric slant columns retrieved using the reference sector method. Figure 4 (top) shows the monthly mean values for February 2005, where a considerable amount of unphysical negative tropospheric NO_2 columns can be identified. Other values may also have errors, but these are less easily identified.

3.2 Stratospheric NO_2 from SCIAMACHY limb and Oslo CTM2

3.2.1 Vertical profiles

As described in Sect. 2.1.2, we extend the SCIAMACHY limb profiles down to the tropopause, using climatological profiles from the Oslo CTM2 simulations for the years 1998–2007. Figure 5 illustrates the validity of this approach, as the profiles measured by SCIAMACHY are similar enough to the climatology of those modelled by Oslo CTM2, especially in the altitude regions between the tropopause and 11 km, where NO_2 concentrations are relatively small.

In some cases, however, the modelled profiles show additional details in the 10–15 km altitude range, which are not detected by the SCIAMACHY sensor. The top right profile in Fig. 5 for example shows a layer of increased NO_2 concentrations around 14 km altitude. This is not a random fluctuation, as the feature is also seen in the climatological model profiles; on the other hand, such sharp peaks are not visible to the SCIAMACHY instrument due to vertical smoothing. At that time of year (early July) and in those latitude regions (65° N), the ECMWF-IFS temperature fields show a layer of enhanced temperature around 14 km. This could drive the decomposition of N_2O_5 and HO_2NO_2, two species which are especially sensitive to temperature changes, leading to increased NO_2 concentrations. Since this feature can be observed in all longitudes, the increased temperature and NO_2 are unlikely to be caused by terrain effects. In these situations, the stratospheric columns resulting from SCIAMACHY observations will be a few percent smaller than those from the model.

3.2.2 Difference to nadir measurements

While the limb and nadir measurements from SCIAMACHY agree quite well qualitatively in unpolluted areas, their quantitative agreement is not perfect, as can be seen in the plots in Sect. 3.2.4. This observation lead us to implement the addition of an offset to the stratospheric slant columns before subtracting them from the measured total columns, as explained in Sect. 2.3.4.

Figure 6 shows the magnitude of the calculated offset in the slant columns over the Pacific Ocean (180° W–150° W). It ranges from $+3 \times 10^{14}$ molec cm^{-2} in near-polar latitudes in December to -4×10^{14} molec cm^{-2} in polar latitudes in austral winter. In the tropics and mid-latitudes, the offset varies between -1×10^{14} and -3×10^{14} molec cm^{-2}, with a minimum in June/July. The same seasonal cycle can be observed in all latitude bands, with minima in June and July, and maxima in December and January.

The VCD_{strat} measured by SCIAMACHY in limb geometry are often larger than those retrieved from nadir measurements. The months November to March show an exemption to this pattern, as can be seen in Fig. 6. Then, nadir columns can be larger than limb columns by about $5–6 \times 10^{14}$ molec cm^{-2} in individual months. This seasonal variation in northern mid- and high latitudes can be explained with the seasonality in tropospheric NO_2 abundances. As the nadir measurements are sensitive to both tropospheric and stratospheric NO_2, any seasonality in tropospheric NO_2 should produce a signal in the offset between limb and nadir measurements. Indeed, Oslo CTM2 simulations show a clear seasonality in tropospheric NO_2 columns with a maximum in boreal winter (see Fig. 20), which is in accordance with the observed seasonality of the offset between limb and nadir measurements. It should however be noted that the offset is also considerably larger in austral summer as compared to austral winter – a difference which probably cannot be explained with tropospheric NO_2 abundances, because according to the used Oslo CTM2 simulations, there is no significant amount of tropospheric NO_2 over the Pacific Ocean in the Southern Hemisphere.

AMTD
5, 5043–5105, 2012

In the tropics, the difference between nadir and limb measurements, if assumed real, could imply that NO_2 abundances in the upper troposphere are significant. This could arise from lightning, or possibly from large scale biomass burning emitted NO_x being transported into the upper atmosphere, and might point towards a source of NO_x for the production of O_3 in the upper troposphere. At higher latitudes, the seasonal variation suggests that in regions where frontal systems are modulating the tropopause height, we might be observing a varying systematic difference between limb and nadir measurements.

While the observed differences are small in absolute numbers and are well within the expected uncertainties of the two measurements, they do have a significant effect on the retrieved tropospheric columns and therefore need to be corrected for. In principle, the offset between nadir and limb measurements could be calculated using measurements from all unpolluted areas (Leue et al., 2001; Bucsela et al., 2006). However, in order to apply the bias correction, accurate knowledge of tropospheric NO_2 abundances is required. The Pacific Ocean, being far away from source regions, is therefore a natural and safe choice throughout the years. While many other ocean regions might often be void of tropospheric NO_2, they are located closer to the continents, and therefore more susceptible to influences from pollution transport events. The Indian and Southern Atlantic Oceans, for example, are sometimes target areas for long-range transport of tropospheric pollution originating from biomass burning events. Therefore, these regions cannot be assumed as always being clean, making them unsuitable for determining the offset between limb and nadir measurements. The Pacific Ocean reference sector therefore remains the only reliable choice.

Overall, further work is needed to investigate this phenomenon in more detail. For this study, an appropriate approach for removing its effect for the study of tropospheric NO_2, which is dominated by lower atmospheric sources and chemical removal of NO_x, has been developed.

AMTD
5, 5043–5105, 2012

3.2.3 Climatological comparison measurement/model

To compare measured and modelled stratospheric NO_2 columns, we calculate their correlation for the five years 2003–2007 for which both measurements and model results are available. Figure 7 shows a scatter plot of the monthly mean values of the VCD_{strat} NO_2 between 60° S and 60° N, interpolated to the locations (and, for the model data, times) of the nadir measurements, and gridded to a 0.125° grid. The Pearson correlation coefficient of the two gridded datasets is 0.974, showing excellent correlation. However, the Oslo CTM2 consistently overestimates the measured NO_2 columns, which can be seen from the slope of 0.94. When all latitudes are considered, the correlation coefficient almost remains unchanged, while the slope of the correlation line decreases to 0.88, showing systematic larger stratospheric NO_2 columns from the model at high latitudes. From the comparison of the measured and modelled vertical profiles, it becomes apparent that the systematic overestimation is mostly coming from altitudes lower than 30 km (see Sect. 3.2.1).

The spatial patterns in VCD_{strat} NO_2 from SCIAMACHY limb measurements and Oslo CTM2 simulations agree remarkably well. Figure 8 shows the average difference between the two datasets for the 2003–2007 period and for three selected climatological monthly means.[2] The difference of the five-year averages has been offset so that it amounts to 0 over the reference sector (180° W–150° W). Systematic differences in the vertical columns are smaller than 5×10^{13} molec cm^{-2}. The spatial pattern of these differences is interesting, showing a clear seasonality and, in many regions, a strong land-sea contrast. One possible explanation might be an orographic effect stemming from the comparably low resolution of the Oslo CTM2. Another possible source for the observed spatial patterns might be the model's treatment of clouds and their influence on photochemistry; in reality, the photochemistry is mostly determined by the short wavelengths which do not penetrate deep enough to be affected by clouds, especially at high latitudes.

[2] See the Supplement for plots of the months not shown in Fig. 8.

AMTD
5, 5043–5105, 2012

The possible influence of clouds has been investigated by filtering for scenes with less than 20 % cloud cover from the FRESCO+ dataset (version 6, Wang et al., 2008). In general, our findings show that clouds cannot be made responsible for the observed land/sea contrast, as most of the spatial patterns do not change qualitatively. The only exceptions are the Antarctic coast, where the cloud-screened data lack the large area of positive differences seen in the full dataset, and the Canadian Hudson Bay area, where the difference in the cloud-screened data turns negative from the positive values in the full dataset. In the case of the Antarctic coast, the large positive differences come mostly from austral spring (September and October). Both effects can, most probably, be attributed to the FRESCO+ cloud algorithm identifying some snow-covered ground scenes as cloudy, which in turn leads to an under-representation of winter values in the climatological average.

The impact of clouds should be explored further, because the understanding of the systematic differences between limb retrievals and model simulations might improve our knowledge of the influence of clouds and surface spectral reflectance on atmospheric photochemistry.

3.2.4 Zonal variability of stratospheric NO_2 columns

A detailed comparison between the two stratospheric datasets has been carried out on the level of monthly averages. Gridded data points have been binned into boxes of 1° longitude × 5° latitude. First, it is noticeable that the zonal variability of SCIAMACHY limb measurements and Oslo CTM2 simulations is remarkably similar (see Fig. 9, top).

At the same time, it becomes clear that the simulated stratospheric columns are often larger than the measured values, which is also shown by the slope 0.88 of the linear fit of the two datasets (see Fig. 7). When matched to the level of the SCIAMACHY nadir measurements over the reference sector by applying a latitude-dependent offset,

Discussion Paper | Discussion Paper | Discussion Paper | Discussion Paper |

AMTD

5, 5043–5105, 2012

Tropospheric NO_2 from SCIAMACHY limb-nadir matching

A. Hilboll et al.

Title Page
Abstract Introduction
Conclusions References
Tables Figures
Back Close
Full Screen / Esc
Printer-friendly Version
Interactive Discussion

the two stratospheric datasets agree reasonably well with the nadir measurements in unpolluted regions (see Fig. 9, centre).[3]

One noticeable feature in all datasets is a systematic low in the observed VCD_{strat} NO_2 over Greenland (∼ 50° W) in autumn, a pattern which can be seen in all observed years 2003–2011 (see Fig. 9). This could be a terrain effect, since the high terrain over Greenland would lead to a higher tropopause and therefore a more shallow stratospheric column. Another possible explanation for this could be the highly complex three-dimensional radiative transfer applying to the limb measurements, which has not been accounted for in the limb profile retrievals (see discussion in Puķīte et al., 2008, and also Sect. 3.5.2).

While, generally, the shape of the zonal variation is very similar between SCIAMACHY limb and Oslo CTM2, in some cases, the amplitudes can differ significantly. Most often, the modelled VCD_{strat} are too high in these situations, sometimes leading to negative tropospheric slant columns when they are being used as stratospheric correction. One exemplary situation is shown in Fig. 10, where, after application of the offset, the agreement between nadir and limb measurements is excellent in those regions without tropospheric pollution. The simulated VCD_{strat}, however, are slightly lower than the measured ones, indicating that probably the model overestimates the stratospheric NO_2 over the reference sector, leading to a too high bias correction.

This points to an operational challenge in applying the offset (see the discussion in Sect. 3.2.2). While the Pacific Ocean region, where the reference sector is located, is the only meridional band which can be assumed to be clear of tropospheric NO_2 pollution, it turns out not to be a fully representative region, which shows e.g. in the maxima of stratospheric NO_2 abundances being located in the reference sector. Reasons for this can be found in the unique geographical conditions: in northern latitudes, it is located over the open ocean and surrounded by the Rocky Mountains in North

[3]To compare SCIAMACHY nadir measurements to the two stratospheric datasets, we applied a stratospheric air mass factor to the total columns measured in nadir geometry. This procedure yields VCD_{strat} NO_2 in those regions without tropospheric pollution.

America and the mountain ranges in East Siberia. This pronounced land-sea contrast strongly influences tropospheric circulation, which in turn might drive stratospheric conditions. The source of the systematic difference between limb and nadir columns might thus be related to NO_2 in the upper troposphere/lower stratosphere (UT/LS) and the tropopause height being modulated by Lee waves which are generated by the wind system and the topography. Figure 10 shows an example where, for the Oslo CTM2 model, the Pacific Ocean is not the most appropriate region to be selected as reference sector for the bias correction.

Furthermore, we show that the assessment of tropospheric pollution can be severely influenced by the used stratospheric correction. Especially over North America, tropospheric columns are strongly influenced by the zonal variability of stratospheric NO_2, because at those latitudes, the zonal gradient between the reference sector and the continent seems to be very pronounced in winter. Figure 11 shows the situation in January 2005 for the latitude band between 50° and 55° N (Southern Canada). In this situation, the stratospheric NO_2 columns over the reference sector are so large that almost everywhere over the North American continent, the resulting SCD_{trop} are negative when using the reference sector method. Only the pollution signal of the cities Montréal, Toronto and Edmonton would be visible as positive tropospheric columns, but the actual VCD_{trop} would be underestimated by more than 50 %. In this example, the limb and Oslo CTM2 stratospheres agree very well.

In very high latitudes, the limb measurements sometimes show significantly less zonal structure than the model simulations or the nadir measurements. Figure 12 shows this for the latitude band between 75° and 80° North, for the months July and September 2003. While the Oslo CTM2 simulations agree remarkably well with the nadir measurements in most places, both following similar strongly pronounced patterns, the limb measurements show considerably less zonal variation. This effect probably results from spatial smoothing, as the individual limb states cover a width of 240 km, which amounts to 10 degrees longitude at 77.5° N.

Discussion Paper | Discussion Paper | Discussion Paper | Discussion Paper |

AMTD

5, 5043–5105, 2012

Tropospheric NO_2 from SCIAMACHY limb-nadir matching

A. Hilboll et al.

Finally, an interesting issue regarding the nadir measurements can be identified by comparing them to limb measurements. In many months, the retrieved nadir columns seem to be lower than the integrated limb stratospheric measurements off the Chilean coast in the East Pacific (~ 75–80° W). As it can be seen in Fig. 13, the VCD_{strat} from nadir measurements are lower than those from limb measurements and model simulations by about 1×10^{14} molec cm^{-2}. In this case, it seems not to be an artefact originating from the reference sector offset, as the nadir measurements are significantly higher than the limb measurements at many other longitudes. This might be a hint leading to issues in the nadir retrieval over clean ocean waters, for example from liquid water absorption or vibrational Raman scattering in water (Vountas et al., 2003; Lerot et al., 2010). A more systematic investigation of this is needed, but outside the scope of this study.

3.2.5 Comparison of the day-to-day variability

Particular attention needs to be paid to the variability of the three stratospheric datasets. The very sparse spatial coverage of the limb measurements can lead to large variability of the interpolated data product. As this would severely impact the usability of this data product for stratospheric correction, we investigate this issue by comparing the variability of the stratospheric vertical columns. For 2005, we calculate daily averages of all data points within 2.5° × 2.5° boxes, located at 180° longitude and nine different latitudes. Figure 14 shows the daily time series. Oslo CTM2 simulations generally yield higher VCD_{strat} NO_2 than SCIAMACHY limb measurements at all latitudes, which in turn are generally larger than the nadir measurements from the same instrument. However, the overall variability of all three datasets is very comparable. As a measure to compare the variabilities of the three datasets, we compute the coefficients of variation c_v.

We calculate daily residuals by subtracting a running 31-day average from the daily time series (see Fig. 15), and define c_v as the ratio of their standard deviation and sample mean (see Table 1).

AMTD

5, 5043–5105, 2012

It becomes apparent that the variability of the three datasets is quite comparable; values for c_v fall within 15 % of each other in most latitude regions. As expected, the variability of measured SCIAMACHY limb columns is often larger than that of Oslo CTM2 columns. However, with the exception of the tropics, where c_v from limb measurements is higher by more than a factor of two, the magnitude of the difference allows to conclude that the measurement noise in individual limb columns, while being significant, does not severely impact the retrieval of tropospheric NO_2 columns. The coefficient of variation c_v of the nadir measurements is larger than that of the limb measurements at almost all latitudes, hinting to higher random errors in the nadir retrieval as compared to the limb retrieval.

3.3 Air mass factor calculations

3.3.1 Influence of using the correct stratospheric NO_2 profile for air mass factor calculations

As described in Sect. 2.3.2, the integrated and interpolated VCD_{strat} need to be converted to slant columns. The simplest approach is to use an air mass factor based on a single atmospheric profile, here the climatological stratospheric NO_2 profile from the U.S. Standard Atmosphere 1976 (Committee on Extension to the Standard Atmosphere, 1976), and to assume a constant surface reflectivity, here 0.05. The influence of the surface reflectivity on the stratospheric AMF is reported to be very low (Wenig et al., 2004), which is why this effect is not further investigated within this study. Figure 16 shows the relative change of the stratospheric AMF introduced by using the actual stratospheric NO_2 profile as measured by SCIAMACHY. In most cases, the actual shape of the stratospheric NO_2 profile only has minor influence on the calculation of stratospheric air mass factors. Replacing the NO_2 vertical profile from the U.S. Standard Atmosphere with the actual profile measured by SCIAMACHY increases the stratospheric air mass factors by 2–5 %.

AMTD
5, 5043–5105, 2012

In austral winter, however, stratospheric air mass factors calculated using NO_2 profiles measured by SCIAMACHY can be up to 60 % larger than those using the U.S. Standard Atmosphere, as small absolute values lead to large relative errors. Here, the SZA is usually large (at 60° S, SCIAMACHY measures around 09:20 LT, which is about 90 min earlier than at 60° N), leading to a higher dependency of the retrieved slant columns on the absorber profile.

3.3.2 Influence of the temperature-dependence of the NO_2 absorption cross-section

The NO_2 absorption cross-section has a well-known dependence on temperature (Burrows et al., 1998). Boersma et al. (2004) have suggested a simple linear approach to correct for this effect in the retrieval of tropospheric NO_2 columns. The NO_2 absorption cross-section used in the DOAS fit was measured at a fixed temperature of 243 K. At very low stratospheric temperatures, the cross-section representing the actual atmospheric conditions is therefore larger than the one used in the retrieval, leading to an overestimation of the stratospheric NO_2 column. This will subsequently be corrected for by an increased air mass factor.[4]

To assess the influence of the temperature-dependence of the NO_2 absorption cross-section on the stratospheric NO_2 correction, we performed a sensitivity study on the seven years of data from 2004 until 2010. Our results show that the temperature dependence of the NO_2 absorption cross-section actually has significant influence on stratospheric air mass factors. As it can be seen in Fig. 17, accounting for the dependence on temperature leads to an increase of the stratospheric air mass factors by between 5 % and 10 %, compared to using a fixed temperature of 243 K. The influence is highest for the winter months and can reach up to 15 % in the climatological mean. Considering the whole dataset from 2004 to 2010, the temperature correction

[4] To be precise, one should speak of pseudo air mass factors when incorporating temperature correction.

AMTD
5, 5043–5105, 2012

amounts to an increase in the air mass factor by 6.4 %, indicating a mean stratospheric temperature lower than 243 K.

3.4 Improvements to the tropospheric data product

When using SCIAMACHY limb measurements or Oslo CTM2 simulations as stratospheric correction scheme instead of the reference sector method, the data quality of the resulting fields of tropospheric slant columns improves considerably. Figure 4 shows SCD_{trop} NO_2 for February 2005, using the reference sector method, SCIAMACHY limb measurements, and Oslo CTM2 simulations as stratospheric correction. Compared to using the reference sector method, both other stratospheric corrections considerably reduce the number of negative tropospheric NO_2 columns.

3.4.1 Time series in regions of interest

Possible improvements to the tropospheric data product can be evaluated by looking at time series over regions where the reference sector method leads to problematic results. Figure 18 shows time series of tropospheric slant columns for the period from October 2002 until May 2011 over four regions with different characteristics. When using the reference sector method for stratospheric correction, the Northern Scandinavia region shows a very clear seasonal cycle, with large negative values in winter. While the large amplitude of the oscillations is mostly due to the varying measurement geometry, the fact that the monthly mean values are consistently negative results from the observation already made in Sect. 3.2.4, where we showed that, especially in polar winter, stratospheric NO_2 fields are far from being zonally homogeneous. Most often, stratospheric NO_2 between 60° N and 75° N seems to peak over the reference sector – a result which is backed by investigation of the zonal variability of the stratospheric NO_2 products (see Sect. 3.2.4). When using SCIAMACHY limb measurements or Oslo CTM2 simulations as stratospheric correction, these issues appear to be solved. The retrieved slant columns show a clear seasonal cycle with large winter maxima, as it is to

Discussion Paper | Discussion Paper | Discussion Paper | Discussion Paper |

AMTD

5, 5043–5105, 2012

Tropospheric NO_2 from SCIAMACHY limb-nadir matching

A. Hilboll et al.

be expected from measurement geometry and enhanced lifetime of tropospheric NO_2 in winter, due to photochemistry. The curves for SCIAMACHY limb and Oslo CTM2 qualitatively agree very well throughout the year, and during summer months, also with the reference sector method.

In the Southern Atlantic region, results are similar. The large amplitudes of the reference sector time series in spring are not present any more when using limb measurements or Oslo CTM2 simulations as stratospheric correction. However, the SCIAMACHY and Oslo CTM2 datasets do not seem to agree as well. This might be due to the fact that the overall magnitude of the tropospheric slant columns is considerably smaller in this region, leading to a higher relative influence of the measurement and modelling uncertainties on the time series.

In the Western Pacific region, a clear seasonal cycle can be seen independently of the used stratospheric correction. During the summer months, all three datasets agree very well. During winter, however, the tropospheric slant columns retrieved using the reference sector method are considerably larger than the other two datasets, by as much as 60 %. This interesting feature might hint towards higher stratospheric NO_2 columns in this region compared to the reference sector, which is directly neighbouring to the east. While this observation is supported by the plots of zonal variability in Sect. 3.2.4, the reason for this repeating pattern is unclear.

Finally, over North America, the situation is more delicate. When using the reference sector method, the time series shows a weak seasonal cycle, with higher values around winter and lower values around summer. When either SCIAMACHY limb measurements or Oslo CTM2 simulations are used as stratospheric correction, however, the seasonal cycle becomes a lot more pronounced. The tropospheric columns in winter more than double in many years, while the summer lows remain almost unchanged. Generally, the seasonal cycle becomes very clearly visible.

AMTD
5, 5043–5105, 2012

3.4.2 Global distribution

When investigating the global distribution of tropospheric NO_2 columns derived using the different stratospheric corrections, several interesting features can be seen. Each October, for instance, tropospheric NO_2 columns retrieved using Oslo CTM2 simulations as stratospheric correction show unreasonably large positive values around the Antarctic coast (see Fig. 19). We believe that this can be explained by stratospheric denitrification processes towards the end of the ozone hole not being correctly represented in the model's chemistry scheme, leading to inaccurate zonal variations in modelled stratospheric NO_2 concentrations.

Occasionally, the use of a certain stratospheric correction scheme can severely influence the interpretation of the data. In October 2005, for example, the SCD_{trop} retrieved using Oslo CTM2 data suggest that a plume of tropospheric NO_2 pollution from South African biomass burning towards the Indian Ocean can be seen (see Fig. 19). When using SCIAMACHY limb measurements as stratospheric correction, however, the same region does not show as distinct features being interpretable as pollution transport. Unfortunately, it cannot be decided which of the two stratospheric corrections leads to a more accurate result in cases like this unless independent validation data are available.

3.4.3 Tropospheric background signal

The calculated climatology of monthly mean values of VCD_{trop} NO_2 over the Pacific Ocean (see Sect. 2.3.5) shows that according to the Oslo CTM2, the assumption of a clean troposphere is mostly valid throughout the year (see Fig. 20). Only in northern mid-latitudes, and there especially during winter, significant amounts of tropospheric NO_2 can be found in the model results. These enhanced NO_2 columns can most probably be attributed to exported pollution from Eastern Asia and North America. Due to the enhanced lifetime of tropospheric NO_2, the modelled columns over the Pacific Ocean are higher during the winter months.

Discussion Paper | Discussion Paper | Discussion Paper | Discussion Paper |

AMTD

5, 5043–5105, 2012

Tropospheric NO_2 from SCIAMACHY limb-nadir matching

A. Hilboll et al.

These findings agree well with the assumptions made in previous studies, which also used CTM output to account for tropospheric NO_2 over the Pacific Ocean (Martin et al., 2002). However, it should be emphasised that no detailed measurements of tropospheric NO_2 concentrations over the Pacific Ocean, covering several latitude bands, exist. The (relatively small) correction of the tropospheric background applied here using the Oslo CTM2 results is therefore not well validated by atmospheric observations.

3.5 Error analysis

3.5.1 Errors in the nadir measurements

Several different sources contribute to the total error in the slant columns measured by SCIAMACHY in nadir geometry. The uncertainties in the measured radiances lead to a random error in the DOAS fitting procedure. Systematic errors can be introduced by the absorption cross-sections used in the DOAS fit. Inaccuracies in the fitting procedure, like e.g. errors in the estimation of water leaving radiance, lead to retrieval errors. In total, these errors amount to approximately 4×10^{14} molec cm^{-2} for the retrieved slant columns, which is less than 5 % (Richter et al., 1998; Boersma et al., 2004; Wenig et al., 2004). Additionally, the nadir columns are subject to errors introduced by air mass factor calculations. For tropospheric columns over polluted regions, this is the dominating error source, which has been discussed elsewhere (Boersma et al., 2004; Leitão et al., 2010; Heckel et al., 2011). Here, only the uncertainties introduced into the stratospheric contribution of the signal are of interest. The vertical NO_2 profiles (taken from the limb measurements) as well as the temperatures from the ERA-Interim reanalysis both contribute to these errors, but are hard to quantify. The sensitivities of the resulting air mass factors to changes in the vertical absorber profile and to the temperature profile are given in Figs. 16 and 17, respectively, showing that the contribution of uncertainties in these two quantities do not contribute significantly to the total error in most cases.

AMTD
5, 5043–5105, 2012

3.5.2 Errors in the limb measurements

Random errors in the measured radiances and systematic errors due to inaccuracies in the used absorption cross-sections can influence the limb retrieval as well as the nadir retrieval. Instrument pointing errors can impact on the vertical resolution and position of the measured profiles, and the retrieval sensitivity decreases at lower altitudes. These error sources are discussed in detail in Bauer et al. (2012) and Rozanov et al. (2005a), and are expected to add up to less than 15 % of the VCD_{strat} in most cases.

In those cases when the tropopause layer lies below the lower boundary of the limb profiles at 11 km, we extend the measured limb profiles with climatological profiles derived from Oslo CTM2 simulations (see Sect. 2.1.2). Errors in the climatological modelled vertical profiles can thus contribute to the total error of the stratospheric columns. However, our comparison of modelled and measured profiles shows that this effect can generally be neglected, as NO_2 number concentrations in the UT/LS region are very low (see Fig. 5).

One further uncertainty comes from the radiative transfer modelling. Air masses from far away can contribute to the limb signal reaching the satellite, and spatial gradients can further complicate the situation. This effect has been studied in great detail in Puķīte et al. (2010). Depending on the tangent height, the errors introduced to the retrieved NO_2 concentrations can be as large as 20 %. Puķīte et al. show that these errors can be avoided by using a tomographic 2-D approach in the radiative transfer calculations. It is however not applicable in an operational data product, as it is only improving the profile retrieval in the case of reduced distance between the individual SCIAMACHY measurements (3.3°) obtained in dedicated limb-only orbits. Based on the findings of Puķīte et al., we estimate the upper bound of the error on the retrieved stratospheric columns to be 30 % in some rare extreme cases of low absolute values, while in most situations, the associated error should not exceed 10 % of the VCD_{strat}.

AMTD
5, 5043–5105, 2012

3.5.3 Errors in the resulting tropospheric slant columns

Uncertainties in the tropospheric slant columns derived by the limb-nadir matching approach are determined by the uncertainties in both the nadir and limb observations as well as the model background added over the Pacific Ocean. Our study suggests that the random error in the stratospheric columns retrieved from limb measurements is of the same magnitude as the one for nadir measurements (see Table 1), leading to squared random errors in the resulting tropospheric slant columns. Assuming a 10 % random uncertainty in the limb columns, and maximum stratospheric slant columns of about 1×10^{16} molec cm^{-2} at latitudes below 60°, errors of up to 1×10^{15} molec cm^{-2} can be introduced. Systematic errors are to a large extent removed by adjusting the limb columns over the reference sector, but longitude dependent offsets between limb and nadir measurements might still exist.

While it is difficult to quantify such uncertainties, a careful study of the climatological differences between measured and modelled stratospheric columns can lead towards a better understanding of problematic regions (see Fig. 8). In early boreal spring, the measured vertical columns are significantly higher than the modelled columns in northern high and mid-latitudes by approx. 3×10^{14} molec cm^{-2}. In July, on the other hand, the measured columns are lower than the modelled ones over almost all of the Eurasian continent by up to 2×10^{14} molec cm^{-2}. Furthermore, the systematic differences exhibit a stripe structure in the subtropics and mid-latitudes between South America and Australia. This feature can influence the interpretation of the tropospheric slant columns, as outlined in Sect. 3.4.2. Likewise, in July, modelled stratospheric columns are significantly higher than measured ones along the western coast of Greenland. This feature can clearly be attributed to the measurements, because the systematic underestimation of the limb-measured columns is also visible in the climatological difference between SCIAMACHY limb and nadir columns (see the Supplement). In October, stratospheric columns modelled by Oslo CTM2 are unreasonably low in the southern polar region. At the same time, a streaky pattern similar to the one observed in July

AMTD
5, 5043–5105, 2012

can be seen over the Indian Ocean; the sign of the differences is however reversed, and their magnitude amounts to up to 2×10^{14} molec cm^{-2}. The impact of these differences on the tropospheric slant columns depends on the corresponding stratospheric air mass factors, which are typically of the order of 2–3 over low and mid-latitudes, but can be as large as 9 at 85° SZA (high latitudes in winter). The systematic differences highlighted above therefore correspond to tropospheric slant column uncertainties of usually up to 5×10^{14} molec cm^{-2}, but can be as large as 2.5×10^{15} molec cm^{-2} at high latitudes in winter.

Over polluted regions, the bulk of tropospheric NO_2 abundances is located in the boundary layer, leading to a one-to-one translation of these systematic errors in the slant columns to errors in the vertical columns, because the tropospheric air mass factor is close to one. In these cases, the uncertainties in the vertical columns only contribute a small relative fraction to the large measured quantities. In cleaner regions, the tropospheric air mass factor is larger than one and approaching the stratospheric AMF, leading to smaller absolute contributions of the stratospheric correction scheme to the total errors in the tropospheric vertical columns. We conclude that in most polluted cases, the relative importance of the error introduced by the limb stratospheric correction is rather small, but care must be taken over clean regions and those areas highlighted above, where model and measurements show larger deviations.

4 Summary and conclusions

In the present study, we implemented the limb-nadir matching method to correct for the stratospheric contribution to total slant columns of NO_2 retrieved using the DOAS technique from SCIAMACHY nadir measurements. The use of SCIAMACHY limb measurements was compared to the simple reference sector method and to using stratospheric NO_2 columns modelled with the Oslo CTM2. In contrast to previous studies, we interpolate one stratospheric NO_2 value for every single nadir-mode measurement made by SCIAMACHY using only the limb data taken in the same orbit. This leads to a very

AMTD
5, 5043–5105, 2012

accurate representation of the zonal variability of stratospheric NO_2, avoiding the problems arising from spatio-temporal averaging. However, this advantage comes at the cost of creating a stratospheric correction method tailor-made for SCIAMACHY nadir measurements – the interpolation scheme described in this study cannot be applied to other satellite sensors like, e.g. GOME-2.

The two stratospheric NO_2 fields from SCIAMACHY limb measurements and Oslo CTM2 simulations were found to agree surprisingly well. The resulting tropospheric NO_2 columns are consequently very similar. Both stratospheric correction methods provide a significant and important improvement compared to the originally used reference sector method. However, both the limb measurements and the modelled columns cannot be applied as an absolute correction. They both need to be corrected for a systematic bias by shifting them to the level of the nadir measurements over a clean region over the Pacific Ocean. For SCIAMACHY limb measurements, Beirle et al. (2010) already faced the same issue. In the case of the Oslo CTM2 simulations, this offset is in principle a very simplistic assimilation scheme. In contrast to the TM4 assimilation used in the retrievals at KNMI (Boersma et al., 2007), our approach is different in that the “assimilation” is not performed online during the model calculations but rather a-posteriori. On the other hand, Oslo CTM2 features a full chemistry scheme compared to the simpler mechanisms found in TM4 (K. F. Boersma, personal communication, 2010). While measurements of NO_2 over the Pacific Ocean are sparse, tropospheric NO_2 abundances must be accounted for in this bias correction. Results from the Oslo CTM2 show that tropospheric NO_2 columns over the reference sector are generally very low, but can reach significant amounts in northern mid-latitudes in winter. Therefore, we have used a climatology based on data from this model to account for the tropospheric background in the data.

The sensitivity of stratospheric air mass factors to actual atmospheric conditions has been analysed as well as the importance of the temperature dependence of the NO_2 absorption cross-section. In most regions, using climatological vertical profiles for the air mass factor calculations introduces errors of less than 2.5 %. Only during the winter

AMTD
5, 5043–5105, 2012

months, applying the U.S. Standard Atmosphere climatological NO_2 profiles results in a significant underestimation of stratospheric AMFs, which in very high southern latitudes can reach up to 60 %. The influence of the temperature dependence of the NO_2 absorption cross-section is more substantial. Using a fixed temperature of 243 K in the DOAS fit leads to an overestimation of stratospheric NO_2 abundances by 6.4 % on average. During winter months, the influence can be as large as 15 % in the climatological means.

The present study reveals many details on the interpretation of the involved datasets, which were found to be in very good agreement with each other. In several cases, shortcomings of the reference sector method can be made up for by applying either the limb or the model correction, significantly improving the consistency of the resulting tropospheric columns. For example, we found that during winter, tropospheric columns are underestimated by a factor of 2 over North America when using the reference sector method. During biomass burning season, the choice of the stratospheric correction scheme can influence whether or not export of tropospheric NO_2 pollution from Africa to the Indian Ocean can be identified in the satellite data.

While it is hard to give a quantification of the error of the resulting tropospheric slant columns, we can conclude that our stratospheric correction scheme, while leading to a squaring of the random error component, minimises the error due to the zonal variability of stratospheric NO_2 fields. When accounting for a systematic bias between the two stratospheric datasets by forcing their difference to be zero over the Pacific Ocean, SCIAMACHY limb measurements and Oslo CTM2 simulations exhibit very good agreement. Climatological differences between the two vertical column datasets are smaller than 2×10^{14} molec cm^{-2} on an annual basis, and in most cases smaller than 3×10^{14} molec cm^{-2} on a monthly basis. However, the lack of independent measurements and thorough validation makes it impossible to say which of the two datasets is more correct. In most cases, uncertainties of the order of magnitude deduced from the observed differences between the two stratospheric corrections result in tropospheric slant column uncertainties of less than 5×10^{14} molec cm^{-2}, but in some rare

AMTD
5, 5043–5105, 2012

cases can be as large as 2.5×10^{15} molec cm^{-2}. While over polluted regions, the stratospheric contribution to the uncertainties can usually be neglected when applying the limb-nadir matching technique, it has to be considered over clean regions, in particular where the agreement between model and measurement is found to be less good.

The limb-nadir matching technique described in this study will be tested for implementation as operational SCIAMACHY NO_2 product in the near future. This approach leads to a significant improvement of the stratospheric correction in the retrieval of tropospheric NO_2 abundances from SCIAMACHY measurements. Modelled stratospheric NO_2 columns from the Oslo CTM2 agree surprisingly well with the measured quantities, and after correcting for the systematic bias over the Pacific Ocean, prove to be a feasible stratospheric correction scheme in cases where limb-nadir matching cannot be applied, e.g. with other satellite sensors.

Finally, this study shows the importance of measuring stratospheric NO_2 accurately for both the interpretation of total column NO_2 and the derivation of tropospheric NO_2 as proposed for SCIAMACHY, and points out limitations of the nadir only observations of GOME, GOME-2, OMI, and related instruments. Limb and occultation measurements of NO_2 are needed to complement the nadir observations to generate an adequate global observing system.

Supplementary material related to this article is available online at: http://www.atmos-meas-tech-discuss.net/5/5043/2012/amtd-5-5043-2012-supplement.pdf.

Acknowledgements. Funding by the Earth System Science Research School (ESSReS), an initiative of the Helmholtz Association of German research centres (HGF) at the Alfred Wegener Institute for Polar and Marine Research, is gratefully acknowledged. The authors further acknowledge funding by the European Union Seventh Framework Programme (FP7/2007-2013) project CityZen (Grant Agreement no. 212095), by the DLR project SADOS (FKZ 50EE0727 and 50EE1105), and by ESA through the SCIAMACHY Quality Working Group.

Øivind Hodnebrog has also received funding from the Research Council of Norway (project no. 188134/E10). Thank you to Steffen Beirle for many fruitful discussions. Tropopause heights have been calculated by Stefan Bötel and Felix Ebojie. SCIAMACHY radiances have been provided by ESA. ECMWF meteorological data were supplied by the European Centre for Medium-Range Weather Forecasts at Reading, UK. Some data used in this study were calculated at German HLRN (High-Performance Computer Center North).

The service charges for this open access publication have been partially covered by the Deutsche Forschungsgemeinschaft (DFG).

References

Bauer, R., Rozanov, A., McLinden, C. A., Gordley, L. L., Lotz, W., Russell III, J. M., Walker, K. A., Zawodny, J. M., Ladstätter-Weißenmayer, A., Bovensmann, H., and Burrows, J. P.: Validation of SCIAMACHY limb NO_2 profiles using solar occultation measurements, Atmos. Meas. Tech., 5, 1059–1084, doi:10.5194/amt-5-1059-2012, 2012. 5051, 5071

Beirle, S., Platt, U., Wenig, M., and Wagner, T.: NO_x production by lightning estimated with GOME, Adv. Space Rese., 34, 793–797, doi:10.1016/j.asr.2003.07.069, 2004. 5045

Beirle, S., Kühl, S., Puķīte, J., and Wagner, T.: Retrieval of tropospheric column densities of NO_2 from combined SCIAMACHY nadir/limb measurements, Atmos. Meas. Tech., 3, 283–299, doi:10.5194/amt-3-283-2010, 2010. 5048, 5050, 5055, 5074

Berntsen, T. K. and Isaksen, I. S. A.: A global three-dimensional chemical transport model for the troposphere 1. Model description and CO and ozone results, J. Geophys. Res., 102, 21239–21280, doi:10.1029/97JD01140, 1997. 5052

Bertram, T. H., Heckel, A., Richter, A., Burrows, J. P., and Cohen, R. C.: Satellite measurements of daily variations in soil NO_x emissions, Geophys. Res. Lett., 32, L24812, doi:10.1029/2005GL024640, 2005. 5045

Bian, H. and Prather, M. J.: Fast-J2: accurate simulation of stratospheric photolysis in global chemical models, J. Atmos. Chem., 41, 281–296, doi:10.1023/A:1014980619462, 2002. 5052

Boersma, K. F., Eskes, H. J., and Brinksma, E. J.: Error analysis for tropospheric NO_2 retrieval from space, J. Geophys. Res., 109, D04311, doi:10.1029/2003JD003962, 2004. 5046, 5049, 5054, 5066, 5070

Boersma, K. F., Eskes, H. J., Veefkind, J. P., Brinksma, E. J., van der A, R. J., Sneep, M., van den Oord, G. H. J., Levelt, P. F., Stammes, P., Gleason, J. F., and Bucsela, E. J.: Near-real time retrieval of tropospheric NO_2 from OMI, Atmos. Chem. Phys., 7, 2103–2118, doi:10.5194/acp-7-2103-2007, 2007. 5045, 5047, 5074

Bogumil, K., Orphal, J., Homann, T., Voigt, S., Spietz, P., Fleischmann, O., Vogel, A., Hartmann, M., Kromminga, H., Bovensmann, H., Frerick, J., and Burrows, J.: Measurements of molecular absorption spectra with the SCIAMACHY pre-flight model: instrument characterization and reference data for atmospheric remote-sensing in the 230–2380 nm region, J. Photochem. Photobiol. A, 157, 167–184, doi:10.1016/S1010-6030(03)00062-5, 2003. 5050

Bovensmann, H., Burrows, J. P., Buchwitz, M., Frerick, F., Noël, S., and Rozanov, V. V.: SCIAMACHY: mission objectives and measurement modes, J. Atmos. Sci., 56, 127–150, doi:10.1175/1520-0469(1999)056<0127:SMOAMM>2.0.CO;2, 1999. 5045, 5047

Brasseur, G. P. and Solomon, S.: Aeronomy of the Middle Atmosphere, 3rd Edn., Springer, 2005. 5046

Bucsela, E. J., Celarier, E. A., Wenig, M. O., Gleason, J. F., Veefkind, J. P., Boersma, K. F., and Brinksma, E. J.: Algorithm for NO_2 vertical column retrieval from the ozone monitoring instrument, IEEE T. Geosci. Remote, 44, 1245–1258, doi:10.1109/TGRS.2005.863715, 2006. 5047, 5059

Burrows, J., Hölzle, E., Goede, A., Visser, H., and Fricke, W.: SCIAMACHY – scanning imaging absorption spectrometer for atmospheric chartography, Acta Astronaut., 35, 445–451, doi:10.1016/0094-5765(94)00278-T, 1995. 5045

Burrows, J. P., Dehn, A., Deters, B., Himmelmann, S., Richter, A., Voigt, S., and Orphal, J.: Atmospheric remote-sensing reference data from GOME: Part 1. Temperature-dependent absorption cross-sections of NO_2 in the 231–794 nm range, J. Quant. Spectrosc. Ra., 60, 1025–1031, doi:10.1016/S0022-4073(97)00197-0, 1998. 5066

Burrows, J. P., Weber, M., Buchwitz, M., Rozanov, V. V., Ladstaetter-Weissenmayer, A., Richter, A., DeBeek, R., Hoogen, R., Bramstedt, K., Eichmann, K., and Eisinger, M.: The global ozone monitoring experiment (GOME): mission concept and first scientific results, J. Atmos. Sci., 56, 151–175, doi:10.1175/1520-0469(1999)056<0151:TGOMEG>2.0.CO;2, 1999. 5045

Burrows, J. P., Platt, U., and Borrell, P.: The Remote Sensing of Tropospheric Composition from Space, 1st Edn., Springer, 2011. 5045

AMTD

5, 5043–5105, 2012

Tropospheric NO_2 from SCIAMACHY limb-nadir matching

A. Hilboll et al.

Callies, J., Corpaccioli, E., Eisinger, M., Hahne, A., and Lefebvre, A.: GOME-2 – Metop's second-generation sensor for operational ozone monitoring, ESA Bull., 102, 28–36, 2000. 5045

Chance, K.: Analysis of BrO measurements from the global ozone monitoring experiment, Geophys. Res. Lett., 25, 3335–3338, doi:10.1029/98GL52359, 1998. 5045, 5050

Committee on Extension to the Standard Atmosphere: U.S. Standard Atmosphere, 1976, US Government Printing Office, Washington, D.C., 1976. 5065

Crutzen, P. J.: The role of NO and NO_2 in the chemistry of the troposphere and stratosphere, Ann. Rev. Earth Planet. Sci., 7, 443–472, 1doi:0.1146/annurev.ea.07.050179.002303, 1979. 5046

de Smedt, I., Stavrakou, T., Müller, J., von der A, R. J., and van Roozendael, M.: Trend detection in satellite observations of formaldehyde tropospheric columns, Geophys. Res. Lett., 37, L18808, doi:10.1029/2010GL044245, 2010. 5045

Dee, D. P., Uppala, S. M., Simmons, A. J., Berrisford, P., Poli, P., Kobayashi, S., Andrae, U., Balmaseda, M. A., Balsamo, G., Bauer, P., Bechtold, P., Beljaars, A. C. M., van de Berg, L., Bidlot, J., Bormann, N., Delsol, C., Dragani, R., Fuentes, M., Geer, A. J., Haimberger, L., Healy, S. B., Hersbach, H., Hólm, E. V., Isaksen, L., Kållberg, P., Köhler, M., Matricardi, M., McNally, A. P., Monge-Sanz, B. M., Morcrette, J., Park, B., Peubey, C., de Rosnay, P., Tavolato, C., Thépaut, J., and Vitart, F.: The ERA-Interim reanalysis: configuration and performance of the data assimilation system, Q. J. Roy. Meteorol. Soc., 137, 553–597, doi:10.1002/qj.828, 2011. 5051, 5054

Dirksen, R. J., Boersma, K. F., Eskes, H. J., Ionov, D. V., Bucsela, E. J., Levelt, P. F., and Kelder, H. M.: Evaluation of stratospheric NO_2 retrieved from the ozone monitoring instrument: intercomparison, diurnal cycle, and trending, J. Geophys. Res., 116, D08305, doi:10.1029/2010JD014943, 2011. 5048

Ebojie, F., von Savigny, C., Ladstätter-Weißenmayer, A., Rozanov, A., Weber, M., Eichmann, K., Bötel, S., Rahpoe, N., Bovensmann, H., and Burrows, J. P.: Seasonal variability of tropospheric oyone derived from SCIAMACHY limb-nadir matching observations, in preparation, 2012. 5051

Gottwald, M. and Bovensmann, H. (Eds.): SCIAMACHY – Exploring the Changing Earth's Atmosphere, Springer Netherlands, Dordrecht, 2011. 5047, 5049

Granier, C., Lamarque, J., Mieville, A., Müller, J., Olivier, J., Orlando, J., Peters, J., Petron, G., Tyndall, G., and Wallens, S.: POET, a database of surface emissions of ozone precursors, available at: http://www.aero.jussieu.fr/projet/ACCENT/POET.php (last access: 11 June 2012), 2005. 5052

Granier, C., Bessagnet, B., Bond, T., D'Angiola, A., Denier van der Gon, H., Frost, G. J., Heil, A., Kaiser, J. W., Kinne, S., Klimont, Z., Kloster, S., Lamarque, J., Liousse, C., Masui, T., Meleux, F., Mieville, A., Ohara, T., Raut, J., Riahi, K., Schultz, M. G., Smith, S. J., Thompson, A., Aardenne, J., Werf, G. R., and Vuuren, D. P.: Evolution of anthropogenic and biomass burning emissions of air pollutants at global and regional scales during the 1980–2010 period, Climatic Change, 109, 163–190, doi:10.1007/s10584-011-0154-1, 2011. 5052

Heckel, A., Kim, S.-W., Frost, G. J., Richter, A., Trainer, M., and Burrows, J. P.: Influence of low spatial resolution a priori data on tropospheric NO_2 satellite retrievals, Atmos. Meas. Tech., 4, 1805–1820, doi:10.5194/amt-4-1805-2011, 2011. 5070

Hesstvedt, E., Hov, Ö., and Isaksen, I. S. A.: Quasi-steady-state approximations in air pollution modeling: comparison of two numerical schemes for oxidant prediction, Int. J. Chem. Kinet., 10, 971–994, doi:10.1002/kin.550100907, 1978. 5052

Heue, K.-P., Richter, A., Bruns, M., Burrows, J. P., v. Friedeburg, C., Platt, U., Pundt, I., Wang, P., and Wagner, T.: Validation of SCIAMACHY tropospheric NO_2-columns with AMAXDOAS measurements, Atmos. Chem. Phys., 5, 1039–1051, doi:10.5194/acp-5-1039-2005, 2005. 5051

Hoinka, K. P.: Statistics of the global tropopause pressure, Mon. Weather Rev., 126, 3303–3325, doi:10.1175/1520-0493(1998)126<3303:SOTGTP>2.0.CO;2, 1998. 5051

Holtslag, A. A. M., De Bruijn, E. I. F., and Pan, H.: A high resolution air mass transformation model for short-range weather forecasting, Mon. Weather Rev., 118, 1561–1575, doi:10.1175/1520-0493(1990)118<1561:AHRAMT>2.0.CO;2, 1990. 5052

Lee, D. S., Köhler, I., Grobler, E., Rohrer, F., Sausen, R., Gallardo-Klenner, L., Olivier, J. G. J., Dentener, F. J., and Bouwman, A. F.: Estimations of global NO_x emissions and their uncertainties, Atmos. Environ., 31, 1735–1749, doi:10.1016/S1352-2310(96)00327-5, 1997. 5045

Leitão, J., Richter, A., Vrekoussis, M., Kokhanovsky, A., Zhang, Q. J., Beekmann, M., and Burrows, J. P.: On the improvement of NO_2 satellite retrievals – aerosol impact on the airmass factors, Atmos. Meas. Tech., 3, 475–493, doi:10.5194/amt-3-475-2010, 2010. 5070

Lerot, C., Stavrakou, T., De Smedt, I., Müller, J., and Van Roozendael, M.: Glyoxal vertical columns from GOME-2 backscattered light measurements and comparisons with a global

model, Atmos. Chem. Phys., 10, 12059–12072, doi:10.5194/acp-10-12059-2010, 2010. 5064
Leue, C., Wenig, M., Wagner, T., Klimm, O., Platt, U., and Jähne, B.: Quantitative analysis of NO_x emissions from Global Ozone Monitoring Experiment satellite image sequences, J. Geophys. Res., 106, 5493–5505, doi:10.1029/2000JD900572, 2001. 5045, 5047, 5059
Levelt, P., van den Oord, G., Dobber, M., Malkki, A., Visser, H., de Vries, J., Stammes, P., Lundell, J., and Saari, H.: The ozone monitoring instrument, IEEE T. Geosci. Remote, 44, 1093–1101, doi:10.1109/TGRS.2006.872333, 2006. 5045
Martin, R. V., Chance, K., Jacob, D. J., Kurosu, T. P., Spurr, R. J. D., Bucsela, E., Gleason, J. F., Palmer, P. I., Bey, I., Fiore, A. M., Li, Q., Yantosca, R. M., and Koelemeijer, R. B. A.: An improved retrieval of tropospheric nitrogen dioxide from GOME, J. Geophys. Res., 107, 4437, doi:10.1029/2001JD001027, 2002. 5045, 5046, 5049, 5056, 5070
Nüß, H., Richter, A., Valks, P., and Burrows, J. P.: Improvements of the NO_2 Total Column Retrieval for GOME-2, O3M SAF Visiting Scientist Activity, Final Report, Universität Bremen, 2006. 5054
Nüß, J. H.: Improvements of the retrieval of tropospheric NO_2 from GOME and SCIAMACHY data, PhD Thesis, University of Bremen, 2005. 5049, 5056
Palmer, P. I., Jacob, D. J., Chance, K., Martin, R. V., Spurr, R. J. D., Kurosu, T. P., Bey, I., Yantosca, R., Fiore, A., and Li, Q.: Air mass factor formulation for spectroscopic measurements from satellites: application to formaldehyde retrievals from the Global Ozone Monitoring Experiment, J. Geophys. Res., 106, 14539–14550, doi:10.1029/2000JD900772, 2001. 5049
Platt, U. and Stutz, J.: Differential Optical Absorption Spectroscopy, Physics of Earth and Space Environments, Springer, Berlin, 2008. 5045, 5050
Platt, U. and Wagner, T.: Satellite mapping of enhanced BrO concentrations in the troposphere, Nature, 395, 486–490, doi:10.1038/26723, 1998. 5045
Prather, M. J.: Numerical advection by conservation of second-order moments, J. Geophys. Res., 91, 6671–6681, doi:10.1029/JD091iD06p06671, 1986. 5052
Price, C., Penner, J., and Prather, M.: NO_x from lightning 1. Global distribution based on lightning physics, J. Geophys. Res., 102, 5929–5941, doi:10.1029/96JD03504, 1997. 5052
Puķīte, J., Kühl, S., Deutschmann, T., Platt, U., and Wagner, T.: Accounting for the effect of horizontal gradients in limb measurements of scattered sunlight, Atmos. Chem. Phys., 8, 3045–3060, doi:10.5194/acp-8-3045-2008, 2008. 5062

AMTD
5, 5043–5105, 2012

Tropospheric NO_2 from SCIAMACHY limb-nadir matching

A. Hilboll et al.

Title Page
Abstract | Introduction
Conclusions | References
Tables | Figures
◀◀ | ▶▶
◀ | ▶
Back | Close
Full Screen / Esc
Printer-friendly Version
Interactive Discussion

Pukīte, J., Kühl, S., Deutschmann, T., Dörner, S., Jöckel, P., Platt, U., and Wagner, T.: The effect of horizontal gradients and spatial measurement resolution on the retrieval of global vertical NO_2 distributions from SCIAMACHY measurements in limb only mode, Atmos. Meas. Tech., 3, 1155–1174, doi:10.5194/amt-3-1155-2010, 2010. 5049, 5071

Richter, A. and Burrows, J. P.: Tropospheric NO_2 from GOME measurements, Adv. Space Res., 29, 1673–1683, doi:10.1016/S0273-1177(02)00100-X, 2002. 5045, 5046, 5050

Richter, A., Wittrock, F., Eisinger, M., and Burrows, J. P.: GOME observations of tropospheric BrO in northern hemispheric spring and summer 1997, Geophys. Res. Lett., 25, 2683–2686, doi:10.1029/98GL52016, 1998. 5045, 5070

Richter, A., DeBeek, R., Fietkau, S., Heckel, A., Löwe, A. G., Medeke, T., Oetjen, H., Weber, M., Wittrock, F., and Burrows, J. P.: Validation von SCIAMACHY level-2 Daten mit bodengebundenen DOAS-Messungen, Tech. Rep., Bremen, 2004. 5051

Richter, A., Burrows, J. P., Nüß, H., Granier, C., and Niemeier, U.: Increase in tropospheric nitrogen dioxide over China observed from space, Nature, 437, 129–132, doi:10.1038/nature04092, 2005. 5047, 5049

Rozanov, A., Bovensmann, H., Bracher, A., Hrechanyy, S., Rozanov, V. V., Sinnhuber, M., Stroh, F., and Burrows, J. P.: NO_2 and BrO vertical profile retrieval from SCIAMACHY limb measurements: sensitivity studies, Adv. Space Res., 36, 846–854, doi:10.1016/j.asr.2005.03.013, 2005a. 5071

Rozanov, A., Rozanov, V. V., Buchwitz, M., Kokhanovsky, A. A., and Burrows, J. P.: SCIATRAN 2.0 – A new radiative transfer model for geophysical applications in the 175-2400 nm spectral region, Adv. Space Res., 36, 1015–1019, doi:10.1016/j.asr.2005.03.012, 2005b. 5054

Schönhardt, A., Richter, A., Wittrock, F., Kirk, H., Oetjen, H., Roscoe, H. K., and Burrows, J. P.: Observations of iodine monoxide columns from satellite, Atmos. Chem. Phys., 8, 637–653, doi:10.5194/acp-8-637-2008, 2008. 5045

Schultz, M. G., Heil, A., Hoelzemann, J. J., Spessa, A., Thonicke, K., Goldammer, J. G., Held, A. C., Pereira, J. M. C., and Bolscher, M. v. h.: Global wildland fire emissions from 1960 to 2000, Global Biogeochem. Cy., 22, GB2002, doi:10.1029/2007GB003031, 2008. 5052

Sierk, B., Richter, A., Rozanov, A., von Savigny, C., Schmoltner, A. M., Buchwitz, M., Bovensmann, H., and Burrows, J. P.: Retrieval and monitoring of atmospheric trace gas concentrations in nadir and limb geometry using the space-borne Sciamachy instrument, Environ. Monit. Assess., 120, 65–77, doi:10.1007/s10661-005-9049-9, 2006. 5048

Sioris, C. E., Kurosu, T. P., Martin, R. V., and Chance, K.: Stratospheric and tropospheric NO_2 observed by SCIAMACHY: first results, Adv. Space Res., 34, 780–785, doi:10.1016/j.asr.2003.08.066, 2004. 5048

Stordal, F., Isaksen, I. S. A., and Horntveth, K.: A diabatic circulation two-dimensional model with photochemistry: simulations of ozone and long-lived tracers with surface sources, J. Geophys. Res., 90, 5757–5776, doi:10.1029/JD090iD03p05757, 1985. 5052

Søvde, O. A., Gauss, M., Smyshlyaev, S. P., and Isaksen, I. S. A.: Evaluation of the chemical transport model Oslo CTM2 with focus on arctic winter ozone depletion, J. Geophys. Res., 113, D09304, doi:10.1029/2007JD009240, 2008. 5052

Tiedtke, M.: A comprehensive mass flux scheme for cumulus parameterization in large-scale models, Mon. Weather Rev., 117, 1779–1800, doi:10.1175/1520-0493(1989)117<1779:ACMFSF>2.0.CO;2, 1989. 5052

van der Werf, G. R., Randerson, J. T., Giglio, L., Collatz, G. J., Kasibhatla, P. S., and Arellano Jr., A. F.: Interannual variability in global biomass burning emissions from 1997 to 2004, Atmos. Chem. Phys., 6, 3423–3441, doi:10.5194/acp-6-3423-2006, 2006. 5052

Vountas, M., Rozanov, V. V., and Burrows, J. P.: Ring effect: impact of rotational Raman scattering on radiative transfer in Earth's atmosphere, J. Quant. Spectrosc. Rad., 60, 943–961, doi:10.1016/S0022-4073(97)00186-6, 1998. 5050

Vountas, M., Richter, A., Wittrock, F., and Burrows, J. P.: Inelastic scattering in ocean water and its impact on trace gas retrievals from satellite data, Atmos. Chem. Phys., 3, 1365–1375, doi:10.5194/acp-3-1365-2003, 2003. 5064

Wang, P., Stammes, P., van der A, R., Pinardi, G., and van Roozendael, M.: FRESCO+: an improved O_2 A-band cloud retrieval algorithm for tropospheric trace gas retrievals, Atmos. Chem. Phys., 8, 6565–6576, doi:10.5194/acp-8-6565-2008, 2008. 5061

Wenig, M., Kühl, S., Beirle, S., Bucsela, E., Jähne, B., Platt, U., Gleason, J., and Wagner, T.: Retrieval and analysis of stratospheric NO_2 from the global ozone monitoring experiment, J. Geophys. Res., 109, D04315, doi:10.1029/2003JD003652, 2004. 5047, 5065, 5070

Wild, O., Zhu, X., and Prather, M. J.: Fast-J: accurate simulation of in- and below-cloud photolysis in tropospheric chemical models, J. Atmos. Chem., 37, 245–282, doi:10.1023/A:1006415919030, 2000. 5052

Williams, E. J., Hutchinson, G. L., and Fehsenfeld, F. C.: NO_x and N_2O emissions from soil, Global Biogeochem. Cy., 6, 351–388, doi:10.1029/92GB02124, 1992. 5045

AMTD

5, 5043–5105, 2012

Tropospheric NO_2 from SCIAMACHY limb-nadir matching

A. Hilboll et al.

Wittrock, F.: The retrieval of oxygenated volatile organic compounds by remote sensing techniques, Ph.D. thesis, Universität Bremen, http://nbn-resolving.de/urn:nbn:de:gbv:46-diss000104818 (last access: 11 June 2012), 2006. 5045

World Meteorological Organization: Scientific Assessment of Ozone Depletion, 2006, Tech. Rep. 50, Geneva, Switzerland, 2007. 5052

Table 1. Coefficients of variation $c_v = \frac{\sigma}{\mu}$ (σ being the standard deviation, and μ being the sample mean) of daily VCD_{strat} NO_2 for nine 2.5° × 2.5° grid boxes located at 180° longitude for the year 2005.

Latitude	SCIA limb	SCIA nadir	Oslo CTM2
−80°	0.290	0.346	0.417
−60°	0.377	0.444	0.409
−40°	0.260	0.305	0.249
−20°	0.142	0.204	0.132
0°	0.084	0.113	0.040
20°	0.156	0.162	0.165
40°	0.253	0.237	0.232
60°	0.420	0.375	0.431
80°	0.271	0.284	0.262

AMTD
5, 5043–5105, 2012

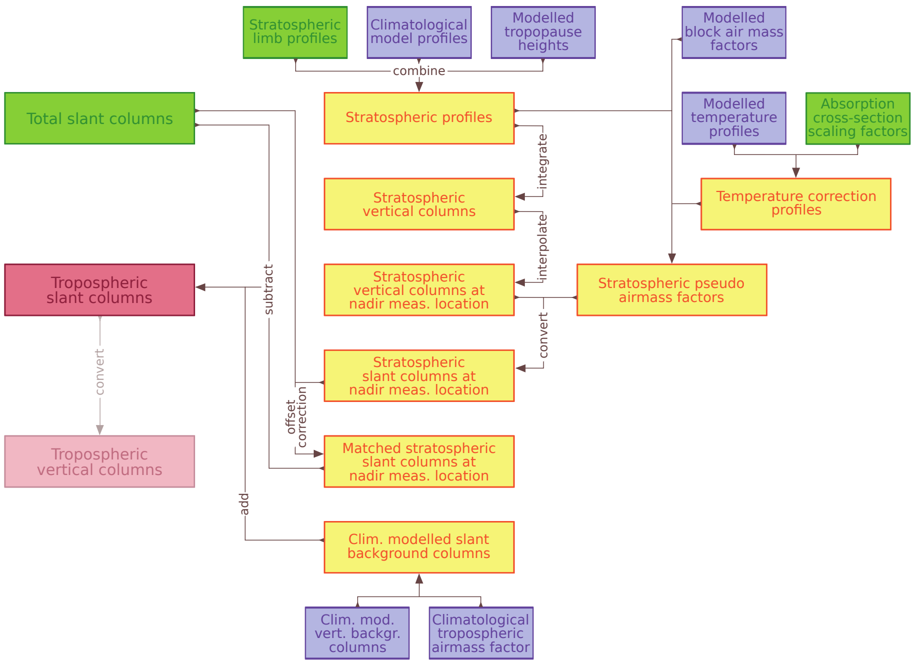

Fig. 1. Data flow of calculating tropospheric NO_2 columns from SCIAMACHY measurements. Measured and modelled quantities are shown in green and purple, respectively, while intermediate results are marked in yellow. Conversion of SCD_{trop} to VCD_{trop} involves calculation of tropospheric air mass factors, the discussion of which is beyond the scope of this study.

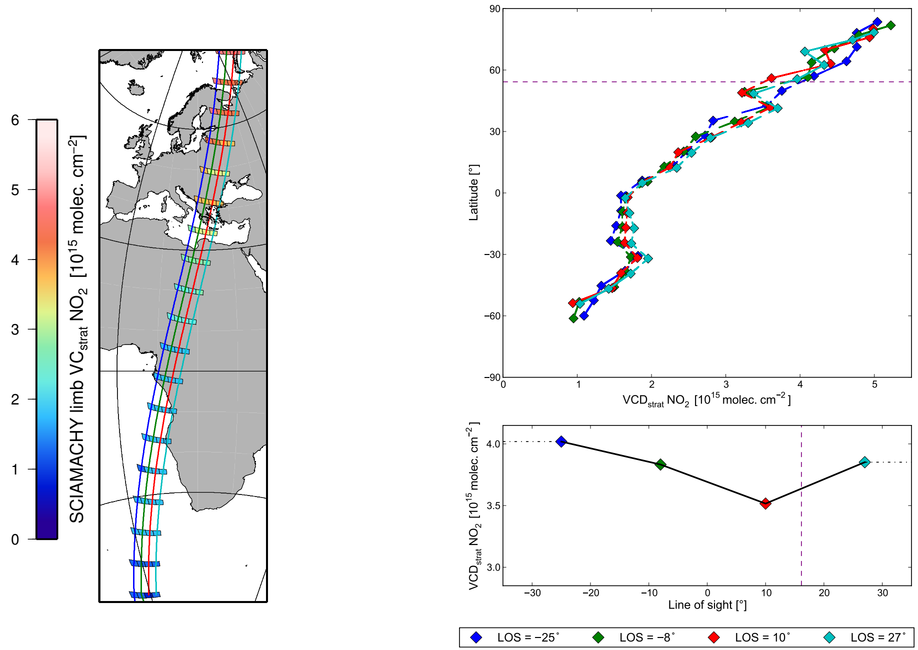

Fig. 2. Interpolation of stratospheric NO_2 columns from SCIAMACHY limb measurements to the location of the same orbit's nadir measurements. As an example, we calculate VCD_{strat} for the nadir measurement located at 54.25° N/32.25° E from SCIAMACHY orbit no. 32984 (21 June 2008). In a first step, each limb state is treated independently. For each state, VCD_{strat} is considered to be a function of latitude only (left). To calculate a VCD_{strat} value for one single nadir measurement, at first, one VCD_{strat} per state is calculated by linear interpolation in latitude (right). Finally, the VCD_{strat} value corresponding to the nadir measurement of interest is calculated by linear interpolation in the line of sight angle (right).

AMTD

5, 5043–5105, 2012

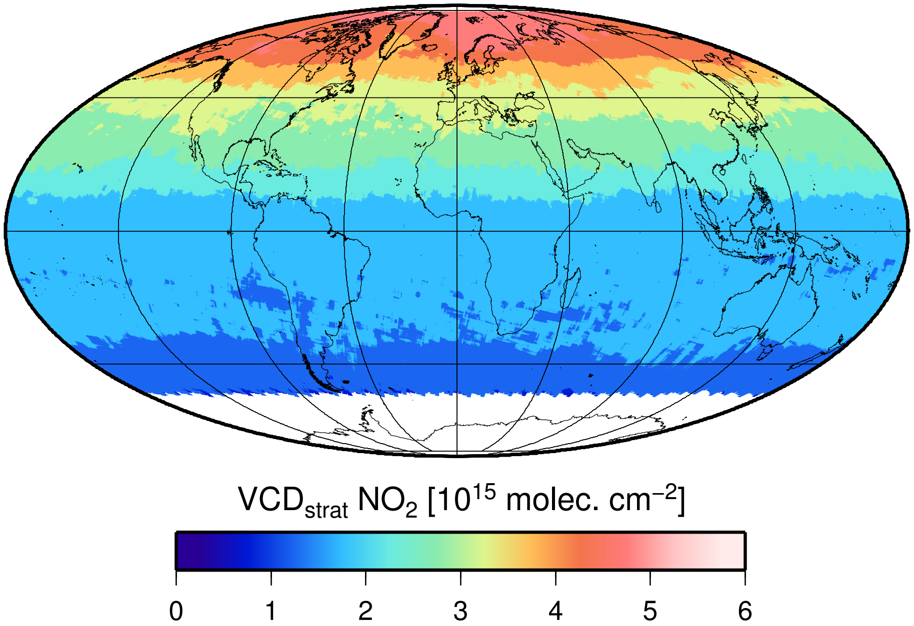

Fig. 3. Monthly averages of VCD$_{strat}$ NO_2 from SCIAMACHY limb measurements for June 2010, interpolated to the locations of the SCIAMACHY nadir measurements, and binned to 0.125°.

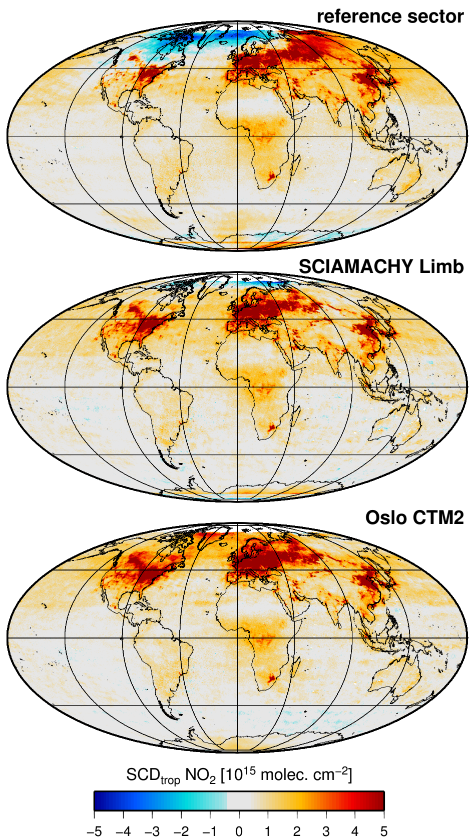

Fig. 4. Monthly average of SCD_{trop} NO_2 from SCIAMACHY for February 2005, using the reference sector method (top), SCIAMACHY limb measurements (centre), and Oslo CTM simulations (bottom) as stratospheric correction.

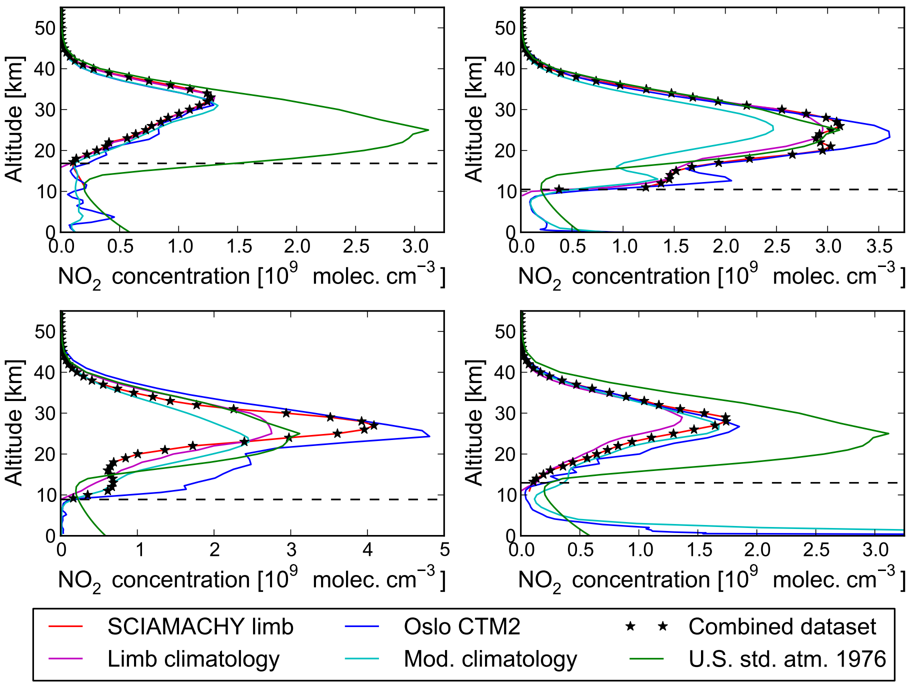

Fig. 5. Vertical NO_2 profiles from SCIAMACHY limb (actual measurement: red, climatology: magenta), Oslo CTM2 (actual value: blue, climatology: cyan), and U.S. Standard Atmosphere 1976 (green) for 1 June 2007, at 3.48° W, 58.66° N (top left), 2 July 2007, at 58.54° W, 63.7° N (top right), 18 February 2007, at 70.54° W, 75.50° S (bottom left), and 27 March 2006, at 5.17° E, 40.65° N (bottom right). The tropopause altitude is shown as a black dashed line, while the combined limb measurements/model climatology profile used for the column and air mass factor calculations in this study are marked as black stars.

AMTD
5, 5043–5105, 2012

Tropospheric NO_2 from SCIAMACHY limb-nadir matching

A. Hilboll et al.

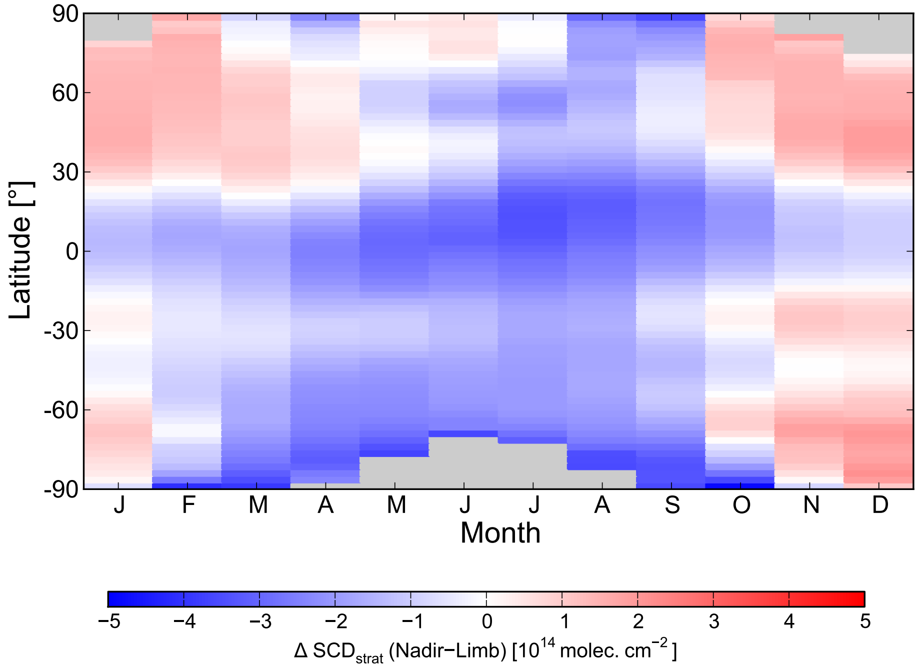

Fig. 6. Monthly climatology of the difference $\Delta SCD_{strat} NO_2$ between SCIAMACHY nadir and limb measurements, averaged from the years 2004–2010. Values have been calculated over the Pacific Ocean (180° W–150° W) and gridded into 2.5° latitude bins.

AMTD
5, 5043–5105, 2012
Tropospheric NO_2 from SCIAMACHY limb-nadir matching
A. Hilboll et al.

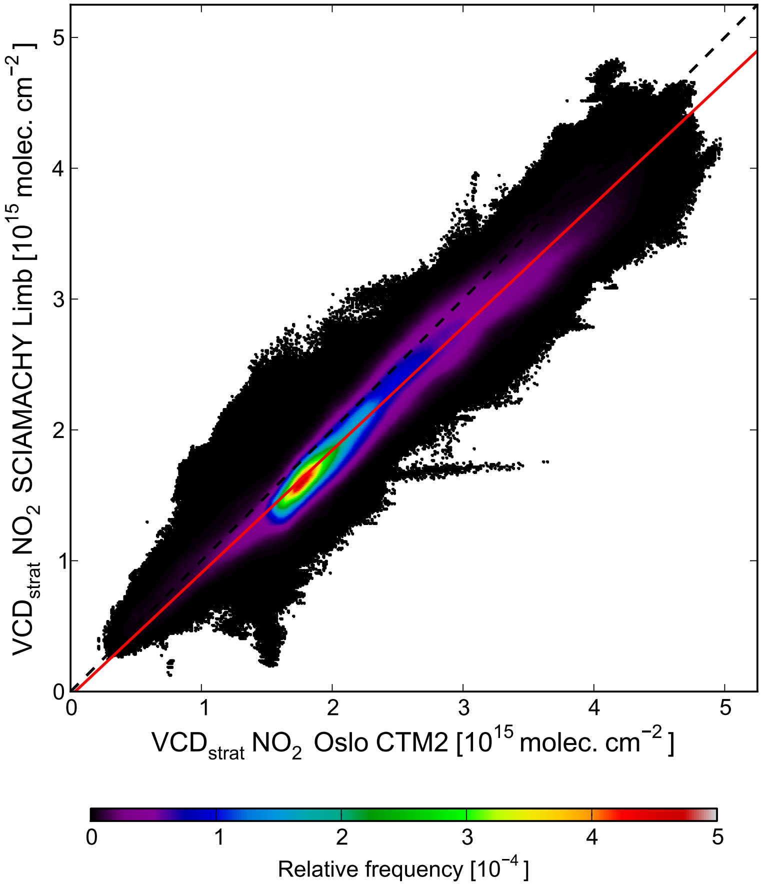

Fig. 7. Scatter plot of monthly mean values for VCD$_{strat}$ NO$_2$ from SCIAMACHY limb measurements and Oslo CTM2 simulations for the 2003–2007 time period, for the latitudes between 60° S and 60° N. The red line marks the linear regression fit (slope 0.94, offset -3.3×10^{13}). The Pearson correlation coefficient of the two datasets is 0.974.

AMTD
5, 5043–5105, 2012

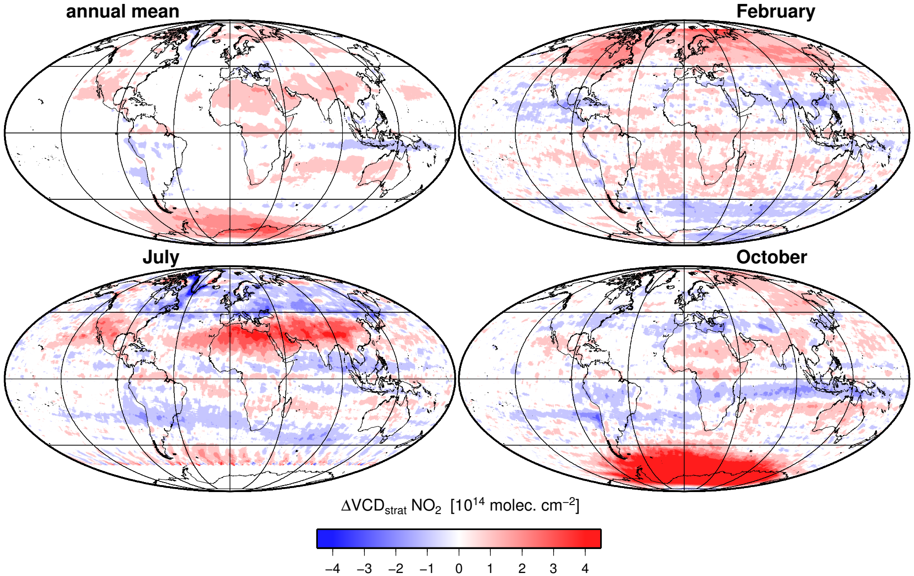

Fig. 8. The difference ΔVCD_{strat} NO_2 between SCIAMACHY limb and Oslo CTM2 for the 2003–2007 time period. Red and blue areas correspond to regions where SCIAMACHY limb measurements are larger and smaller than Oslo CTM2 simulations, respectively. Top left: average difference over all months. Top right: average difference of all Februaries. Bottom left: average difference of all Julies. Bottom right: average difference of all Octobers. An additive offset has been applied to force the difference to equal zero over the reference sector (180° W–150° W).

AMTD
5, 5043–5105, 2012

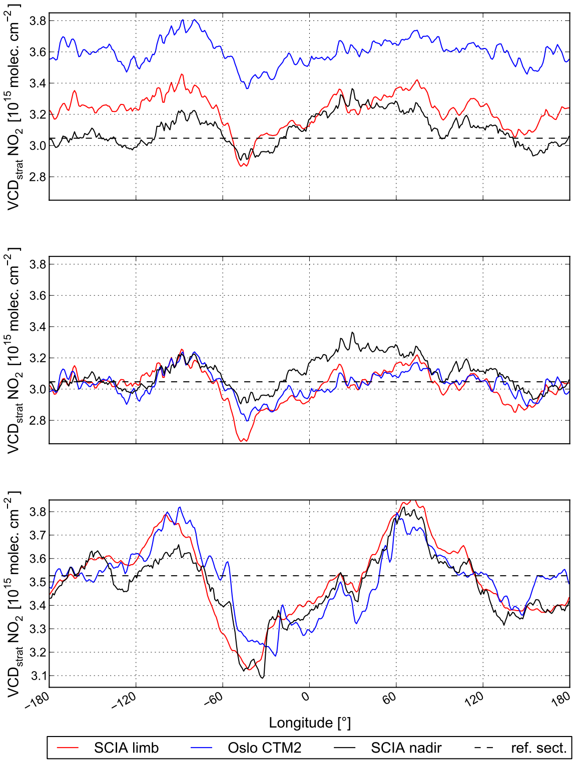

Fig. 9. Zonal variation of VCD$_{strat}$ NO$_2$ from SCIAMACHY limb measurements (red), Oslo CTM2 simulations (blue), and of VCD$_{tot}$ NO$_2$ from SCIAMACHY nadir measurements (stratospheric air mass factor applied, black). The nadir measurements' value over the reference sector is marked as dashed black line. Monthly mean values for September 2006, between 60° and 65° N, "raw" measurements (top) and matched to the nadir measurements over the reference sector (centre), as well as between 70° and 75° N, matched (bottom).

AMTD

5, 5043–5105, 2012

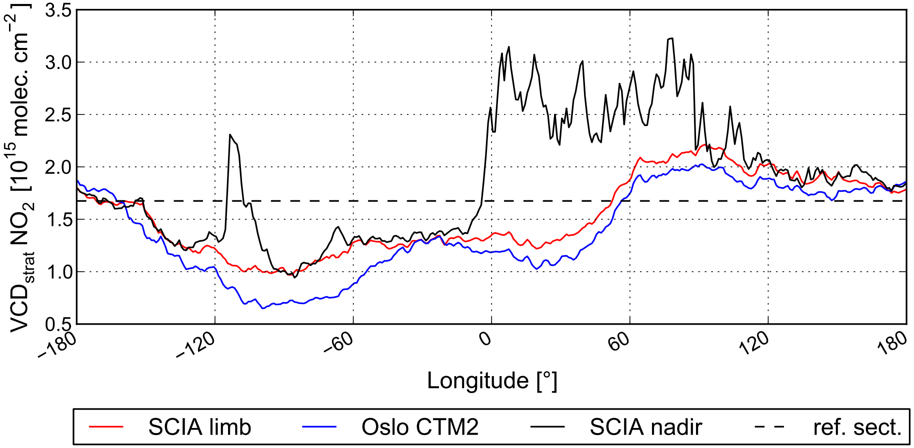

Fig. 10. Zonal variation of VCD_{strat} NO_2 from SCIAMACHY limb measurements (red), Oslo CTM2 simulations (blue), and of VCD_{tot} NO_2 from SCIAMACHY nadir measurements (stratospheric air mass factor applied, black). The nadir measurements' value over the reference sector is marked as dashed black line. Monthly mean values for March 2005, between 60° and 65° N, matched to the level of the nadir measurements over the reference sector.

AMTD

5, 5043–5105, 2012

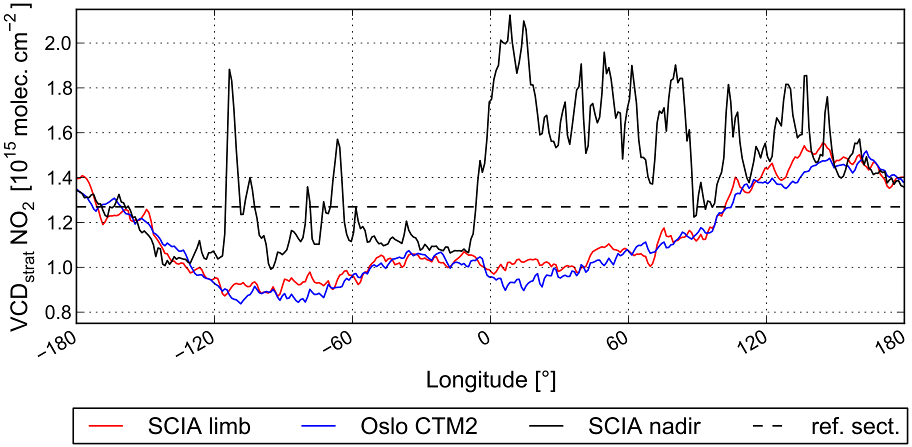

Fig. 11. Zonal variation of VCD_{strat} NO_2 from SCIAMACHY limb measurements (red), Oslo CTM2 simulations (blue), and of VCD_{tot} NO_2 from SCIAMACHY nadir measurements (stratospheric air mass factor applied, black). The nadir measurements' value over the reference sector is marked as dashed black line. Monthly mean values for January 2005, between 50° and 55° N, matched to the level of the nadir measurements over the reference sector.

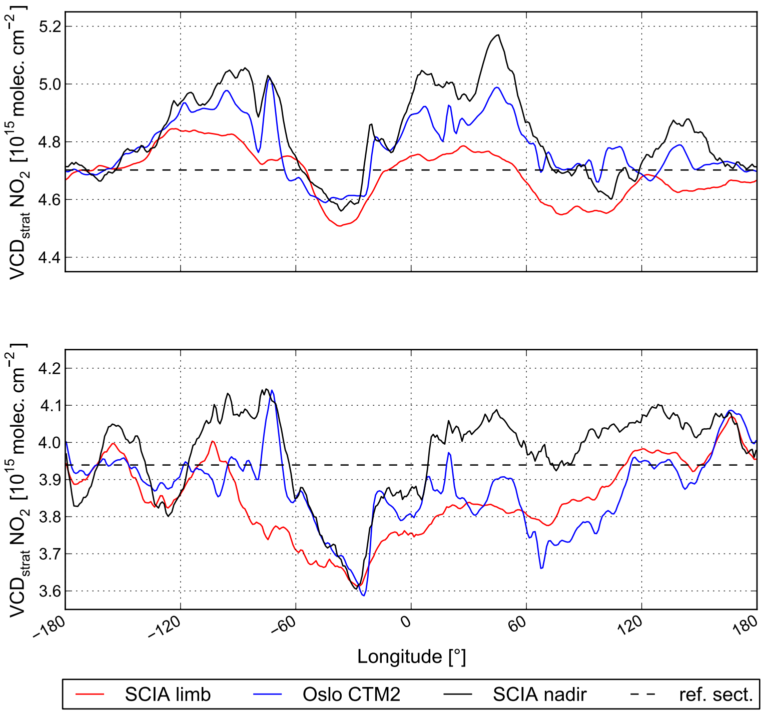

Fig. 12. Zonal variation of VCD_{strat} NO_2 from SCIAMACHY limb measurements (red), Oslo CTM2 simulations (blue), and of VCD_{tot} NO_2 from SCIAMACHY nadir measurements (stratospheric air mass factor applied, black). The nadir measurements' value over the reference sector is marked as dashed black line. Monthly mean values for July (top) and September (bottom) 2003, between 75° and 80° N, matched to the level of the nadir measurements over the reference sector.

AMTD
5, 5043–5105, 2012

Title Page
Abstract | Introduction
Conclusions | References
Tables | Figures
◀| |▶
◀ ▶
Back | Close
Full Screen / Esc
Printer-friendly Version
Interactive Discussion

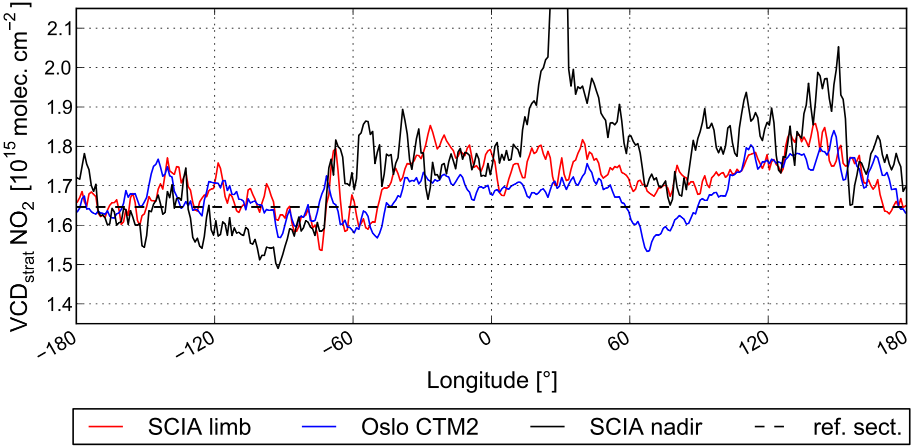

Fig. 13. Zonal variation of VCD_{strat} NO_2 from SCIAMACHY limb measurements (red), Oslo CTM2 simulations (blue), and of VCD_{tot} NO_2 from SCIAMACHY nadir measurements (stratospheric air mass factor applied, black). The nadir measurements' value over the reference sector is marked as dashed black line. Monthly mean values for May 2005, between 30° and 25° S, matched to the level of the nadir measurements over the reference sector.

AMTD
5, 5043–5105, 2012

Tropospheric NO_2 from SCIAMACHY limb-nadir matching

A. Hilboll et al.

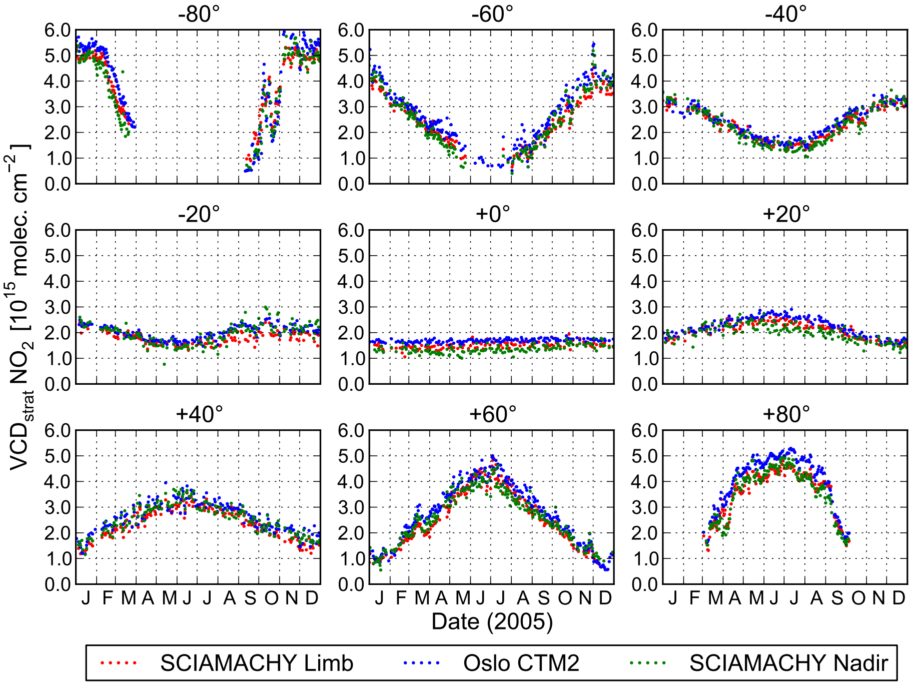

Fig. 14. Daily time series for the year 2005 of VCD_{strat} NO_2 from SCIAMACHY limb (red), Oslo CTM2 (blue), and of VCD_{tot} from SCIAMACHY nadir (stratospheric air mass factor applied, green) for nine 2.5° × 2.5° grid boxes. The centres of the grid boxes are located at 180° longitude and the latitudes are given in the plot titles.

AMTD
5, 5043–5105, 2012

Tropospheric NO_2 from SCIAMACHY limb-nadir matching

A. Hilboll et al.

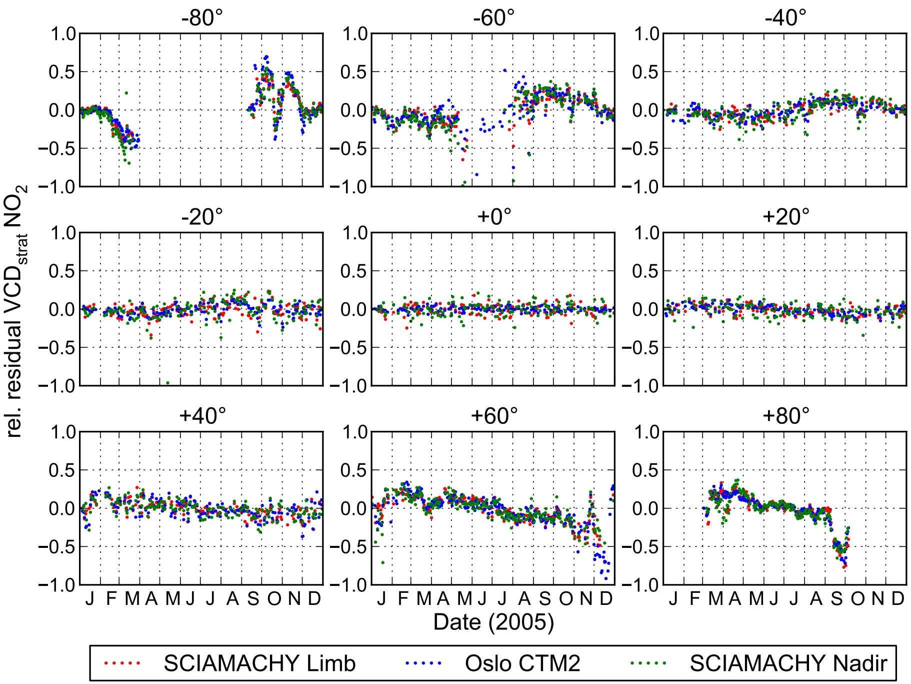

Fig. 15. Time series for the year 2005 of the relative residuals of VCD$_{strat}$ NO_2 from SCIAMACHY limb (red), Oslo CTM2 (blue), and of VCD$_{tot}$ from SCIAMACHY nadir (stratospheric air mass factor applied; green) for nine 2.5° × 2.5° grid boxes. The centres of the grid boxes are located at 180° longitude and the latitudes are given in the plot titles. The residuals have been computed by subtracting a running 31-day average from the daily dataset.

AMTD
5, 5043–5105, 2012

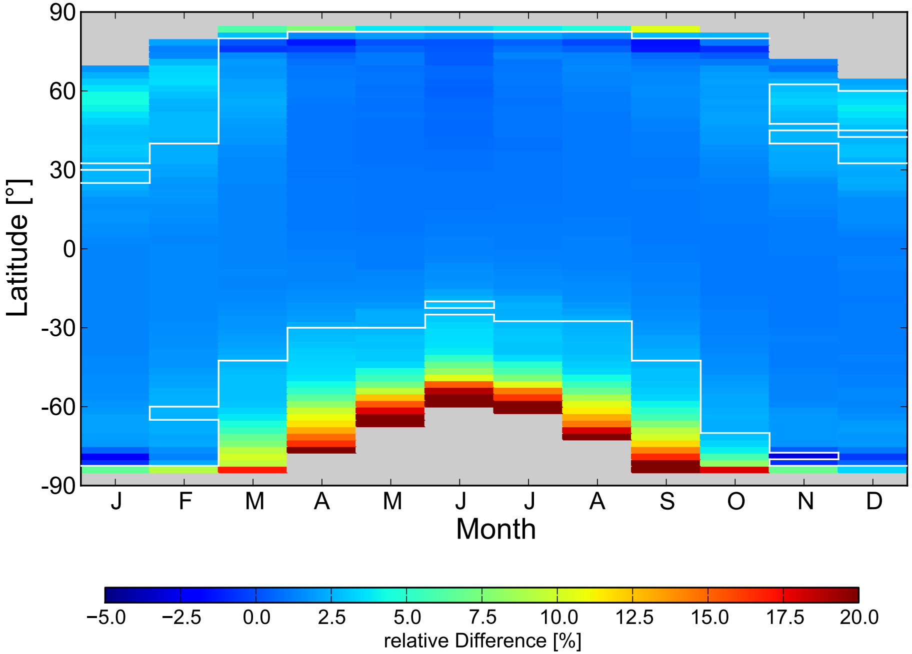

Fig. 16. Monthly climatology of the relative difference between the stratospheric air mass factor calculated using NO_2 vertical profiles from SCIAMACHY limb measurements and the U.S. Standard Atmosphere, calculated for the years 2004–2010. The white line indicates the regions of ±2.5 % relative difference.

AMTD
5, 5043–5105, 2012

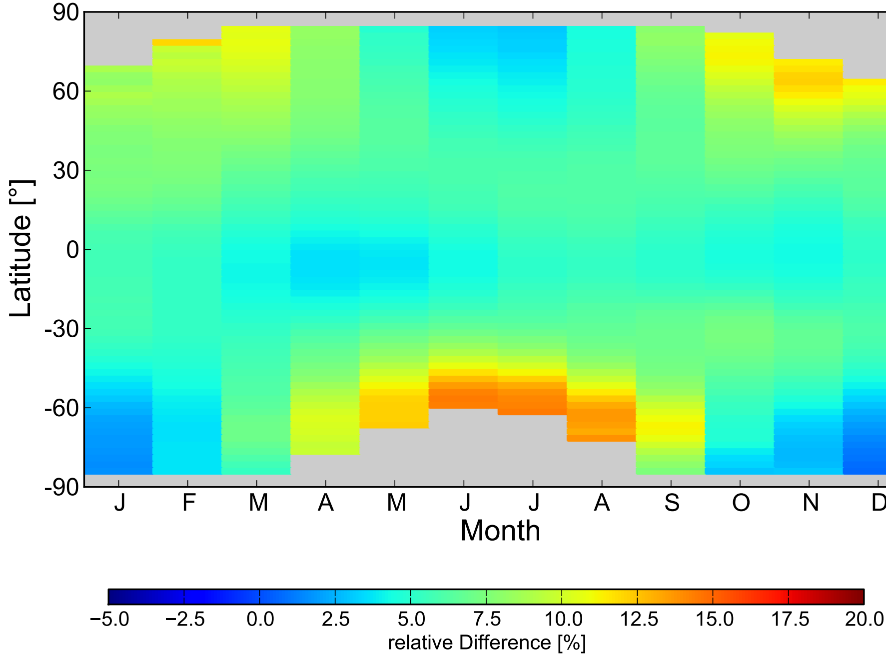

Fig. 17. Monthly climatology of the relative difference between the stratospheric air mass factor calculated using NO_2 vertical profiles from SCIAMACHY limb measurements, corrected for the temperature dependence of the NO_2 absorption cross-section, compared to those determined when using a fixed temperature of 243 K, calculated for the years 2004–2010.

AMTD
5, 5043–5105, 2012

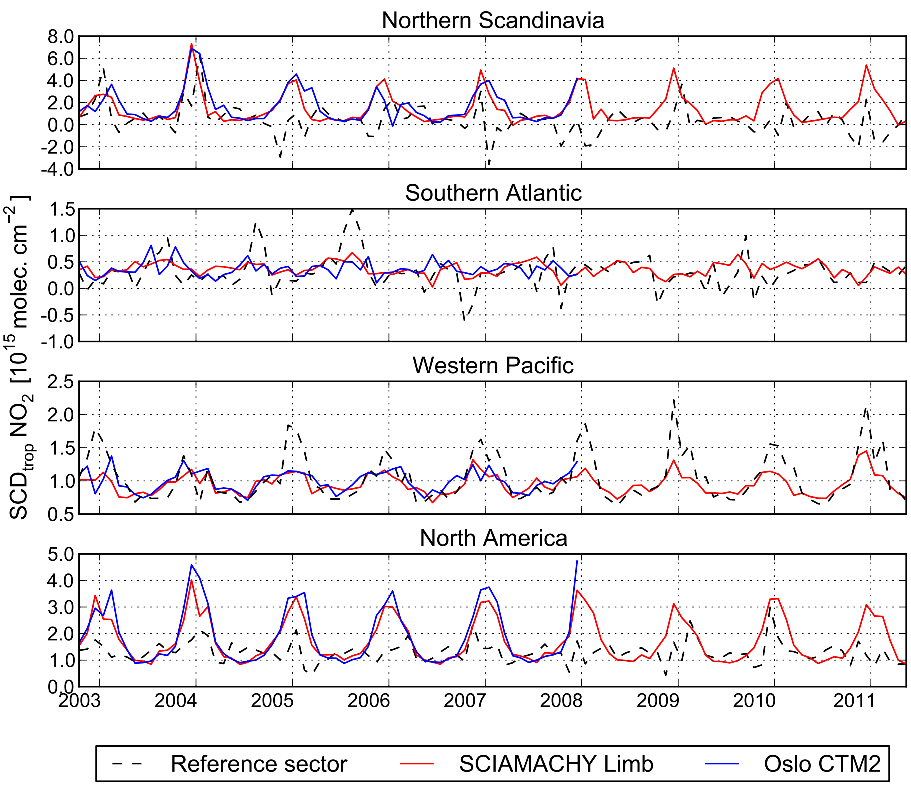

Fig. 18. Time series of monthly mean values of SCD_{trop} NO_2 for the regions Northern Scandinavia (60° N–75° N, 0°–40° E), Southern Atlantic (50° S–30° S, 45° W–15° E), Western Pacific (25° N–50° N, 148° E–178° E), and North America (40° N–60° N, 120° W–90 ° W). Three different stratospheric corrections have been used: SCIAMACHY limb measurements (red), Oslo CTM2 simulations (blue, only until 2007), and the reference sector method (black).

AMTD
5, 5043–5105, 2012

Tropospheric NO_2 from SCIAMACHY limb-nadir matching

A. Hilboll et al.

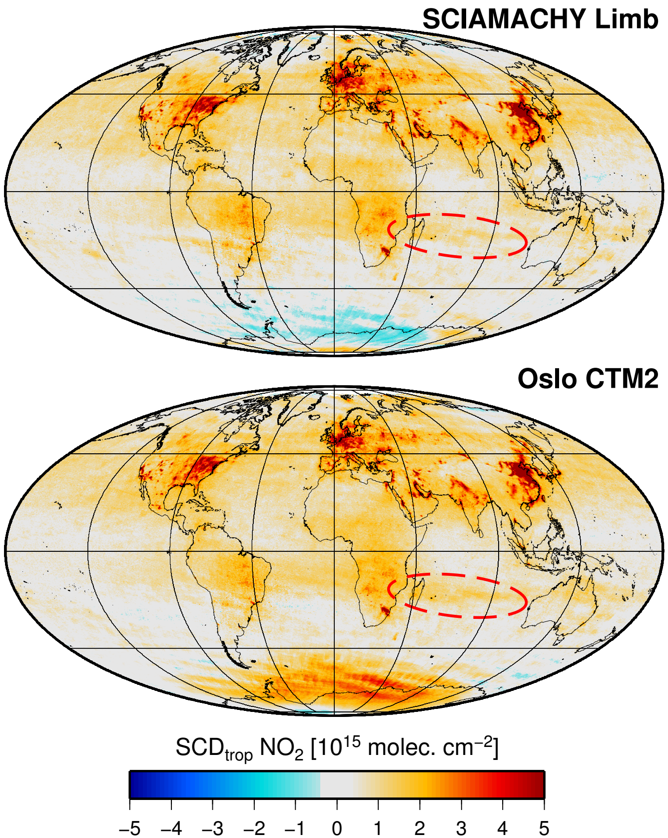

Fig. 19. Monthly average of SCD_{trop} NO_2 from SCIAMACHY for October 2005, using SCIAMACHY limb measurements (top) and Oslo CTM simulations (bottom) as stratospheric correction.

AMTD
5, 5043–5105, 2012

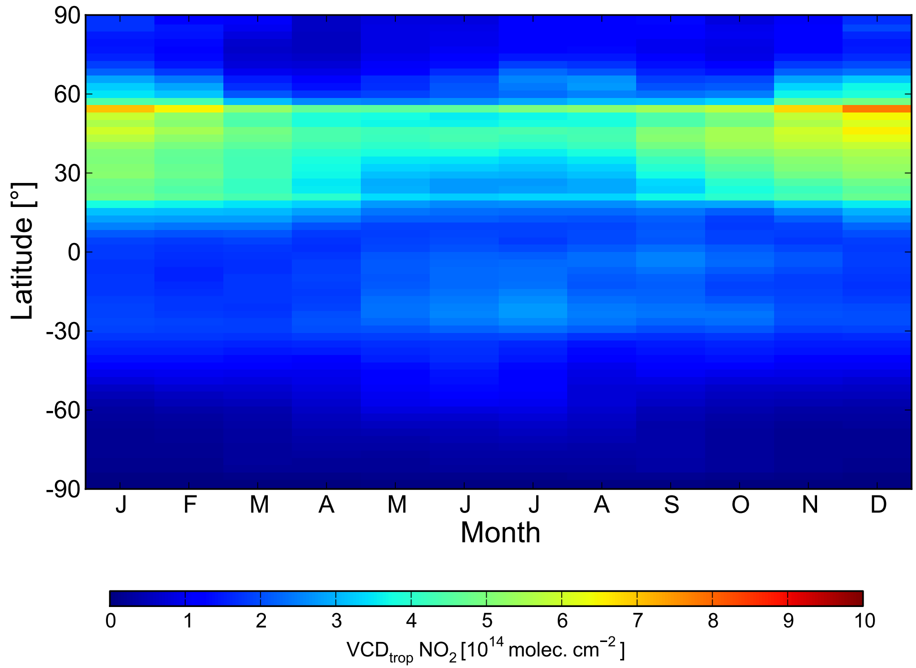

Fig. 20. Climatology of VCD$_{trop}$ NO_2 over the Pacific Ocean (180° W–150° W) for the years 1998–2007, computed from Oslo CTM2 simulations.

AMTD
5, 5043–5105, 2012